69-17,820

BURCHETT, Olden Lee, 1934-

AN EVALUATION OF A LATERALLY CONFINED ISOTHERMAL TEST TECHNIQUE TO ESTIMATE THE SHOCK BEHAVIOR OF LOW-STRENGTH MATERIALS.

The University of Oklahoma, D.Eng., 1969
Engineering, mechanical

University Microfilms, Inc., Ann Arbor, Michigan

THE UNIVERSITY OF OKLAHOMA

GRADUATE COLLEGE

AN EVALUATION OF A LATERALLY CONFINED ISOTHERMAL TEST TECHNIQUE TO ESTIMATE THE SHOCK BEHAVIOR OF LOW-STRENGTH MATERIALS

A DISSERTATION

SUBMITTED TO THE GRADUATE FACULTY

in partial fulfillment of the requirements for the

degree of

DOCTOR OF ENGINEERING

BY

OLDEN L. BURCHETT

Norman, Oklahoma

1969

AN EVALUATION OF A LATERALLY CONFINED ISOTHERMAL TEST TECHNIQUE TO ESTIMATE THE SHOCK BEHAVIOR OF LOW-STRENGTH MATERIALS

APPROVED BY

Charles W. Bert

Franklin J. Appl

[illegible]

[illegible]

William N. Huff

DISSERTATION COMMITTEE

ACKNOWLEDGMENT

The financial aid provided the author by Sandia Laboratories Doctoral Study Program is very much appreciated. Many people assisted the author with his graduate studies and dissertation. The author acknowledges the cooperation and encouragement he received from his wife and family. The author gratefully acknowledges the valuable counsel provided by his advisor, Professor C. W. Bert, and the assistance of Ray Dunaway in assembling the data acquisition system, of Frank Batchelor and Ed Young in running the tests, of Lessie Lee and Emily Young in reducing the experimental data and Maxine Lucas and Bonnie Sharp in preparing and typing the manuscript.

TABLE OF CONTENTS

LIST OF TABLES

LIST OF ILLUSTRATIONS

LIST OF ILLUSTRATIONS

LIST OF SYMBOLS

A = the symbol for the pressure derivative of the initial bulk modulus of a test specimen in the least-squares fitting routines (in Chapter V)

A_1, A_2 = the Grüneisen coefficients

B = the symbol for the initial bulk modulus of a test specimen in the least-squares fitting routines (in Chapter V)

B_S = the adiabatic bulk modulus

B_{SO} = the initial adiabatic bulk modulus

B_T = the isothermal bulk modulus

B_{TO} = the initial isothermal bulk modulus

B' = the first pressure derivative of the bulk modulus

B'' = the second pressure derivative of the bulk modulus

B''' = the third pressure derivative of the bulk modulus

B'''' = the fourth pressure derivative of the bulk modulus

C = the least-squares residual

C_P = the specific heat at constant pressure

C_V = the specific heat at constant volume

D = the axial deformation of the specimen

D^* = the corresponding digital value of the axial deformation of the specimen

D_O^* = the corresponding digital value of the zero axial deformation of the specimen

E = the specific internal energy

E_h = the Hugoniot specific internal energy

E_O = the initial specific internal energy

E_R = the reference specific internal energy

E_T = the specific internal energy due to thermal lattice vibration

E_V = the specific internal energy due to lattice distortion

$\bar{E}$ = Young's modulus of the constraint cylinder and loading rams

F = the axial friction force on the specimen

F^* = the corresponding digital value of the axial friction force on the specimen

F_0^* = the corresponding digital value of the zero axial friction force on the specimen

F^{**} = the average normalized friction force

$G(\xi)$ = the first Fürth volume function

$H(\xi)$ = the second Fürth volume function

K = the Fürth lattice function

L_0 = the initial specimen length

L_1 = the upper loading ram initial length

L_2 = the lower loading ram initial length

ΔL = the corrected one-dimensional-strain deformation of specimen

ΔL_1 = the upper loading ram deformation

ΔL_2 = the lower loading ram deformation

P, P_n = the pressure or the normal pressure or stress

P_a = the adiabatic pressure

P_h = the Hugoniot pressure

P_i = the isothermal pressure

P_0 = the initial pressure

P_R = the reference pressure

P_T = the pressure due to thermal lattice vibration

P_V = the pressure due to lattice distortion

R = the universal gas constant (in Chapter II)

R = the symbol for the pressure derivative of the initial bulk modulus of a specimen series composite in the least-squares fitting routine (in Chapter V)

S = the specific entropy (in Chapter II and III)

S = the symbol for the initial bulk modulus of a specimen series composite in the least-squares fitting routine (in Chapter V)

$\bar{S}$ = the difference of the Fürth exponents

T = the absolute temperature of the specimen (in Chapters II and III)

T = the total applied specimen force (in Chapter V)

T_g = the absolute glass transition temperature

T_h = the Hugoniot absolute temperature of the specimen (in Chapters II and III)

T_0 = the initial absolute temperature of the specimen (in Chapters II and III)

T^* = the corresponding digital value of the total applied specimen force (in Chapter V)

T_o^* = the corresponding digital value of the zero total applied specimen force (in Chapter V)

U = the shock velocity

U_o = the initial shock velocity

V = the Duvall volume function

$V_1(v)$ = the first Duvall volume function

$V_2(v)$ = the second Duvall volume function

V^* = the corrected specimen volume

a = a Fürth constant

a_0, a_1, a_2 = the isentropic equation of state constants

b = a Fürth constant

b_0, b_1, b_2 = the coefficients for a parabolic shock velocity-particle velocity relationship

c = a Fürth constant

c_D = the deformation conversion constant

c_F = the friction force conversion constant

c_T = the total applied force conversion constant

d = the loading ram diameter

d_i = the constraint cylinder inside diameter

d_o = the constraint cylinder outside diameter

m = a Fürth exponent

$\bar{m}$ = a Whitaker - Grisky constant

n = a Fürth exponent

$\bar{n}$ = a Whitaker - Grisky constant

s = the slope of the linear shock velocity - particle velocity relation

u = the particle velocity

u_{fs} = the free surface particle velocity

$u_1, u_2, u_3, u_4, u_5, u_6, u_7, u_8, u_9, u_{10}, u_{11}$ = parameters of the least-squares fitting routine (in Chapter V)

v = the specific volume

v_o = the initial specific volume

$\bar{v}_o$ = the specific volume at zero absolute pressure and temperature

v' = the first pressure derivative of the specific volume

v'' = the second pressure derivative of the specific volume

v''' = the third pressure derivative of the specific volume

v'''' = the fourth pressure derivative of the specific volume

x = the axial specimen variable measured from the bottom end of the specimen

β = the thermal coefficient of volume expansion

β_0 = the initial thermal coefficient of volume expansion

γ = the Grüneisen ratio

ϵ = the one-dimension strain

η = the dimensionless volume variable

Λ = the heat of sublimation

ν = Poisson's ratio of the constraint cylinder and loading rams

ξ = the dimensionless Fürth volume variable

ξ_0 = the initial dimensionless Fürth volume variable

ρ = the material density

ρ_0 = the initial material density

AN EVALUATION OF A LATERALLY CONFINED ISOTHERMAL TEST TECHNIQUE TO ESTIMATE THE SHOCK BEHAVIOR OF LOW-STRENGTH MATERIALS

CHAPTER I.

INTRODUCTION

This investigation was concerned with the feasibility of using isothermal pressure-volume data from laterally confined compression tests to obtain the low-pressure (< 10 kbar) shock Hugoniots of low-strength polymeric materials. Results of laterally confined compression tests on polymethylmethacrylate (PMMA) specimens were expressed in terms of the pressure increase, $P - P_0$, the initial isothermal bulk modulus, B_{T0}, the pressure derivative of the initial isothermal bulk modulus, B'_{T0}, and the ratio of the initial to the final specific volume, v_0/v, with the isothermal Murnaghan equation of state,

$$P - P_0 = \left(B_{T0}/B'_{T0}\right)\left[\left(v_0/v\right)^{B'_{T0}} - 1\right] \qquad (1.1)$$

and then transformed with a technique described by Duvall,[1,2] to obtain the shock Hugoniot. Attention was concentrated on the effects

---

[1] G. E. Duvall and B. J. Zwolinski, Entropic Equations of State and Their Application to Shock Pheromena in Solids, J. Acoust. Soc. Am., 27 (1955), 1054-58.

[2] G. E. Duvall, Pressure-Volume Relations in Solids, J. Appl. Phys., 26 (1957), 235-38.

of test specimen geometry and the friction forces due to lateral constraint.

The interest in determining the shock Hugoniot of a material by transforming isothermal pressure-volume data was prompted by the need for a simple screening test that could be used to evaluate the shock response of large groups of low-strength materials. Such a screening test could be used to determine the two or three most likely candidates from a large group of materials for a particular shock environment application. Then the difficult and extensive shock measurements necessary to define the candidate's shock behavior would be made.

An indirect technique of obtaining the isothermal equation of state has been outlined by Overton[3] and Anderson,[4] and utilized the ultrasonically determined isothermal bulk modulus and its pressure derivative to establish the constant coefficients of the equation of state. The Hugoniot states could then be obtained with the Mie-Grüneisen equation of state[5] or the Duvall transformation.

The two commonly used methods of measuring the pressure-volume behavior of solid materials have been well documented by Bridgman[6] and

---

[3]W. C. Overton, Jr., Relation Between Ultrasonically Measured Properties and the Coefficients in the Solid Equation of State, J. Chem. Phys., 37 (1962), 116-19.

[4]O. L. Anderson, The Use of Ultrasonic Measurements Under Modest Pressure to Estimate Compression at High Pressure, J. Phys. Chem. Solids, 27 (1966), 547-65.

[5]M. H. Rice, R. G. McQueen, and J. M. Walsh, Compression of Solids by Strong Shock Waves, in Solid State Physics, Vol. 6 edited by Seitz and Turnbull. New York: Academic Press, 1958.

[6]P. W. Bridgman, The Physics of High Pressures. London, England: Bell and Sons, 1949.

others. In one method, the specimen was contained in a high-pressure cell and the specimen's volume change and the corresponding pressure was measured. The pressure cell method was used by Bridgman to make accurate pressure-volume measurements. The laterally confined compression test method has been used by Stevens[7] after calibration with gold as the standard material. The specimen volume and the applied pressure were determined by measuring the loading ram force and the relative displacement between the loading rams. Both methods are limited to pressures less than 30 kbar. This study concentrated on the laterally confined compression test method since it was potentially the simplest and least expensive of the three prominent methods of determining the isothermal equation of state.

---

[7]D. R. Stephens and E. M. Lilley, Compression of Isotropic Lithium Hydrides, J. Appl. Phys., 39 (1968), 177-80.

CHAPTER II.

PROBLEM BACKGROUND

The description of the propagation of plane shock waves through solids is similar to the ideal fluid description. Because the solid material can support shear, the shock pressure, P, must be replaced by the stress, P_n, normal to the shock front.[8] Jump conditions representing conservation of mass, momentum and energy, relate the initial state, density ρ_0, pressure P_0, and specific internal energy E_0, to the shocked state, density ρ, pressure P, and specific internal energy E, give

$$\rho = \rho_0 \left[U/(U-u) \right] \qquad \text{(mass conservation)} \qquad (2.1)$$

$$P - P_0 = \rho_0 U u \qquad \text{(momentum conservation)} \qquad (2.2)$$

$$\left(P - P_0\right) u = \rho_0 U \left(E - E_0 + u^2/2\right). \qquad \text{(energy conservation)} \qquad (2.3)$$

The shock velocity is U and the particle velocity imparted to the material by the shock wave is u. These equations are called the Rankine-Hugoniot relations and assume a strain-rate-insensitive, single-phase material without shear strength. Elimination of the shock velocity and the particle velocity from equation (2.3) gives a

---

[8] G. E. Duvall, Some Properties and Applications of Shock Waves, in Response of Metals to High Velocity Deformation, edited by Shewmon and Zackay. New York: Interscience, 1961.

useful form

$$E - E_o = \left(1/2\right)\left(P + B_b\right)\left(v_b - v\right), \quad v_o = 1/\rho_o, \; v = 1/\rho \tag{2.4}$$

where v_o and v are the specific volumes of the material's initial and shock states.

Since five unknown parameters, ρ, P, E, U and u are present in the three Rankine-Hugoniot relations, another independent equation is required if the measurement of one of the parameters is to permit the calculation of the other four parameters. A relationship between the shock velocity and the particle velocity can be determined experimentally by measuring the shock and particle velocities at a sufficient number of points in the shock velocity-particle velocity plane. The relationship usually has the linear form[9]

$$U = U(u) = U_o + s\,u \tag{2.5}$$

When this linear shock velocity-particle velocity relation, equation (2.5), is combined with the Rankine-Hugoniot equations, the shock and particle velocities become

$$U = U_o/\left[1 - s\left(\rho - \rho_o\right)/\rho\right] = U_o/\left(1 - s\eta\right) \tag{2.6}$$

$$u = \left[U_o\left(\rho - \rho_o\right)/\rho\right]/\left[1 - s\left(\rho - \rho_o\right)/\rho\right] = \eta U_o/\left(1 - s\eta\right) \tag{2.7}$$

and the momentum and energy equations are

$$P - P_o = \left[\rho_o U_o^2\left(\rho - \rho_o\right)/\rho\right]/\left[1 - s\left(\rho - \rho_o\right)/\rho\right] = \rho_o U_o^2 \eta/\left(1 - s\eta\right)^2 \tag{2.8}$$

---

[9] G. E. Duvall and G. R. Fowles, Shock Waves, in High Pressure Physics and Chemistry, Vol. 2, edited by R. S. Bradley. New York: Academic Press, 1962.

$$E - E_o = (1/2)U_o\left[(\rho - \rho_o)/\rho\right]^2 / \left[1 - s\,(\rho - \rho_o)/\rho\right]^2 = (1/2)\left[U_o\eta/(1 - s\eta)\right]^2 \qquad (2.9)$$

with the dimensionless volume variable, η, determined by

$$\eta = \Delta v/v_o = (v_o - v)/v_o = (\rho - \rho_o)/\rho \qquad (2.10)$$

Equation (2.8) is the locus of the pressure-specific volume states obtainable by shock transition from the initial pressure-specific volume state and is defined as the Hugoniot. The change in specific internal energy accompanying the shock transition from the initial state is given by equation (2.9). Figure 2.1 shows the Hugoniot states and a typical shock loading path (Rayleigh line) prescribed by

$$(P - P_o)/(v_o - v) = U^2/v_o^2 \ . \qquad (2.11)$$

This equation of the Rayleigh line is obtained by combining equations (2.1) and (2.2).

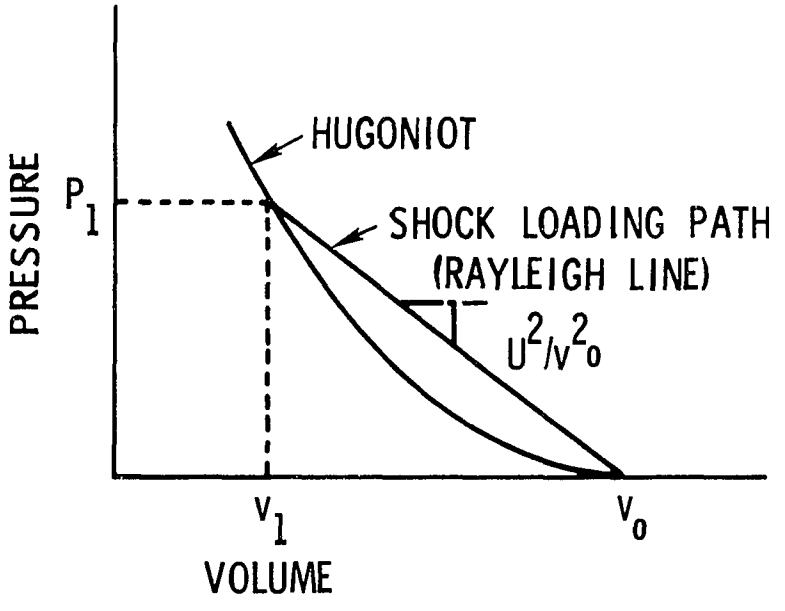

Figure 2.1 Typical Shock Loading Path

Shock interactions resulting from shock waves striking interfaces or other shock waves will change the state of the material. Additional shock loading is governed by the Rankine-Hugoniot relations and the shock velocity-particle velocity relation. Since rarefaction waves cannot exist in single-phase materials,[10] unloading occurs gradually along an isentropic path. The shock state changes can be observed in the pressure-particle-velocity plane. Alternate forms of the Rankine-Hugoniot equations are

$$u - u_o = \pm\left[\left(P - P_o\right)\left(v_o - v\right)\right]^{1/2} \tag{2.12}$$

$$U = v_o\left[\left(P - P_o\right)\left(v_o - v\right)\right]^{1/2} \tag{2.13}$$

$$E - E_o = \left(1/2\right)\left(P + P_o\right)\left(v_o - v\right) \tag{2.14}$$

When the shock velocity is a function of the particle velocity, the pressure-particle velocity representation of the Hugoniot can be expressed as

$$P - P_o = \rho_o u\, U(u) \tag{2.15}$$

The loci of states in the pressure-particle velocity plane that can be reached from a state, (P_1, u_1) are shown in Figure 2.2. Curve E B is the reflection Hugoniot, the mirror image of the Hugoniot, curve E C. The rarefaction isentropes are the curves E A and E D and are obtained from the Riemann integral

$$u - u_1 = \pm \int_{P_1}^{P} \left(-\partial v/\partial P\right)_s^{1/2} dP. \tag{2.16}$$

---

[10] W. E. Drummond, Explosive Induced Shock Waves, Part I. Plane Shock Waves, J. Appl. Phys., 28 (1957), 1437.

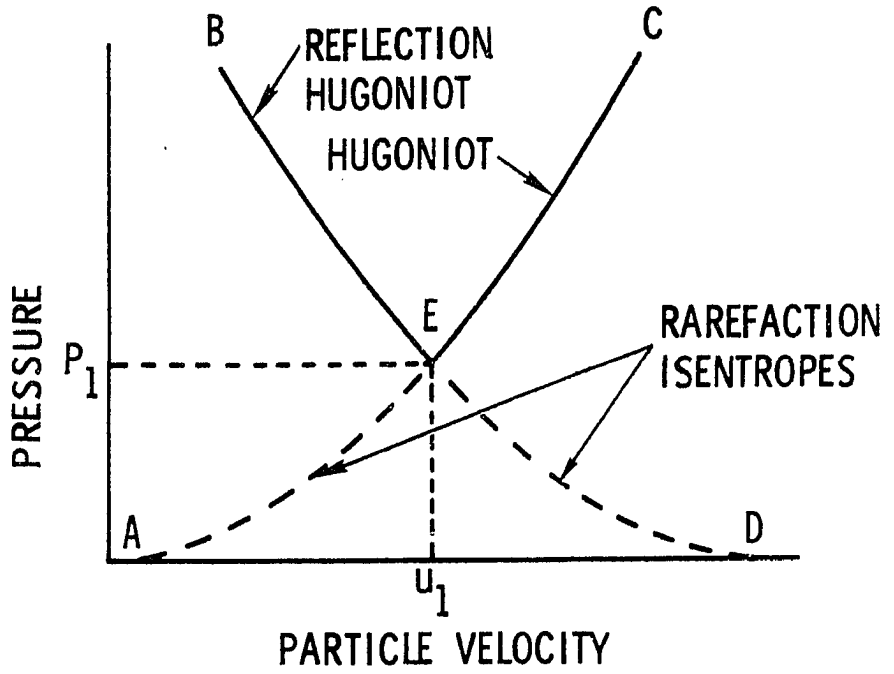

Figure 2.2 Shock States in the Pressure-Particle Velocity Plane

A good estimate of the rarefaction isentrope can be obtained by extending the reflection Hugoniot to negative values of the pressure ($P - P_1$) so that the reflection Hugoniot-isentrope is very nearly the mirror image of the Hugoniot through point (P_1, u_1) about a straight line through the point and normal to the particle velocity axis.[11]

The essential difference between the Hugoniot and the isentrope is that during the shock loading irreversible thermodynamic processes occur in the shock front and produce more heat than if a reversible isentropic loading process was used (see Figure 2.3). Both the initial state and the final Hugoniot state resulting from the shock transition are equilibrium states; therefore, the increase in entropy associated with the Hugoniot must occur in a unique manner. Since the initial

---

[11] Duvall, "Some Properties and..."

and final states of the shocked material defined by the Rankine-Hugoniot equations are equilibrium states, the locus of these equilibrium states form a reversible path. The Hugoniot is this path; therefore, reversible thermodynamics applies to the Hugoniot as well as the isentrope.

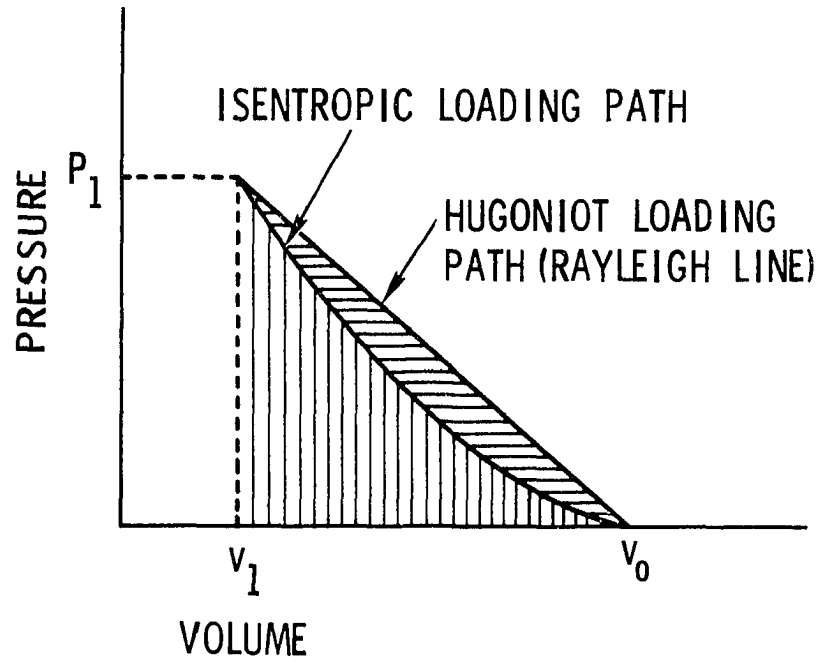

Figure 2.3 Comparison of Hugoniot and Isentropic Loading Paths

Combining and applying the first and second laws[12]

$$dE = TdS - Pdv, \tag{2.17}$$

to the Hugoniot and the isentrope gives

$$TdS = C_v dT + T\left(\gamma/v\right) C_v dv \tag{2.18}$$

and

$$dT/T = -\left(\gamma/v\right) dv. \tag{2.19}$$

Where C_v is the specific heat at constant volume and γ is the

---

[12] Duvall and Zwolinski, "Entropic Equations of..."

Grüneisen ratio,[13,14]

$$\gamma = v \left(\partial P/\partial E\right)_v \quad . \tag{2.20}$$

Measurement of a material's shock response can be made with a variety of experimental techniques.

The shock measurements must be made in the plane-wave region and must not affect the parameters that are to be measured. The plane-wave condition can be maintained at material interfaces if the geometry of the experiment is carefully designed. Shock waves can be produced in a material by the detonation of an explosive that is in direct contact with the material[15,16] or by impacting the material with a flying projectile plate.[17] The shock parameters that are measured usually are the shock velocity and the particle velocity. Such measurements are made over a finite area of a material interface; therefore, certain material surface and shock wave conditions must be met if the measurements are to be accurate. These conditions are: the material surface must be flat and parallel to the shock front and the shock front in the measurement area must be plane.

The shock velocity is determined by time required for the shock

---

[13] J. C. Slater, Introduction to Chemical Physics. New York: McGraw-Hill, 1939.

[14] M. Born and K. Huang, Dynamic Theory of Crystal Lattices. Oxford: Clarendon Press, 1954.

[15] Rice, McQueen and Walsh, "Compression of Solids ..."

[16] J. S. Koehler and G. E. Duvall, Shock Wave Data and the Closed Shell Repulsive Potential in the Noble Metals, Bull. Am. Phys. Soc. Ser. II, 4 (1959), 283.

[17] L. M. Barker and R. E. Hollenbach, System for Measuring the Dynamic Properties of Materials, Rev. Sci. Instrum., 35 (1964), 742-6.

wave to travel a known distance in the material. Shorting pins, optical devices and contact transducers are used to signal the shock arrival at the different points in the material. Measurement of the particle velocity at a free surface requires knowledge of the interaction of the shock wave with the free surface interface. Figure 2.4 illustrates two typical shock wave interface interactions that are encountered in shock wave experiments: the free surface interaction and the interface interaction between two different materials.

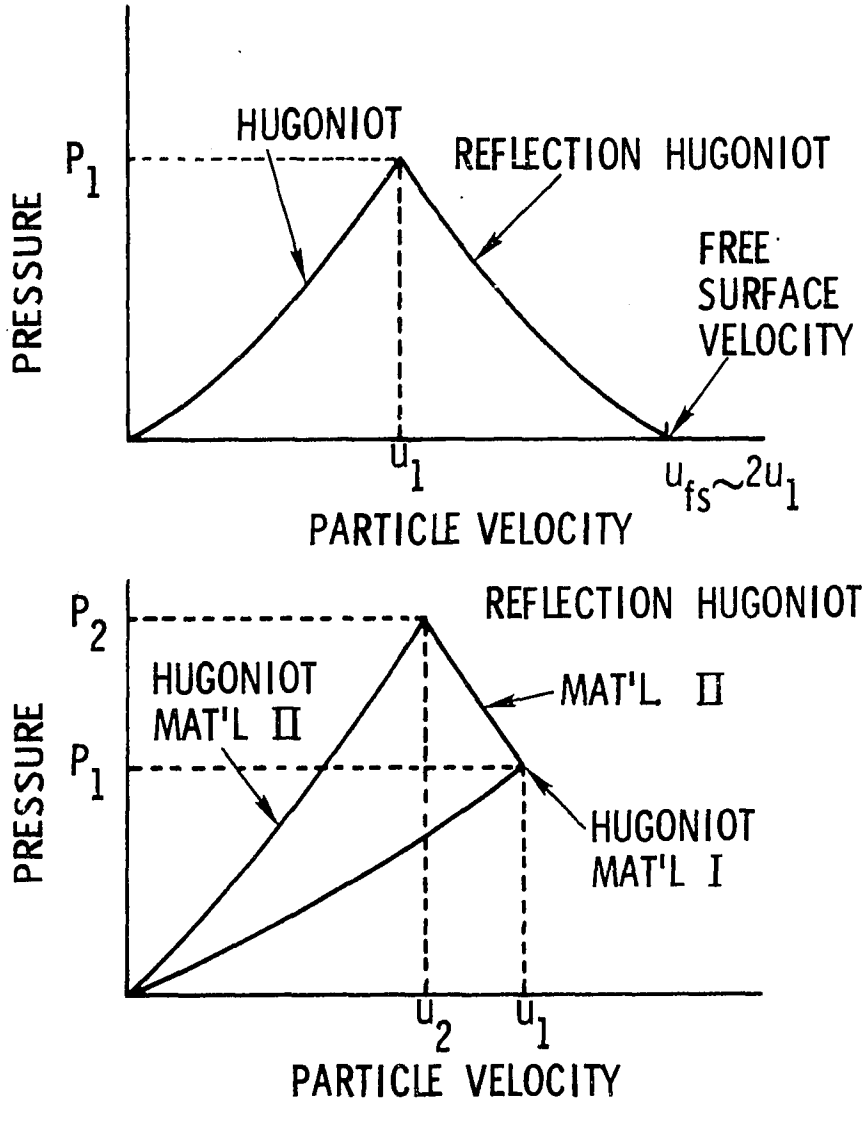

Figure 2.4 Shock Wave Interactions

Figure 2.4a is the basis of the free surface approximation of the particle velocity which gives

$$u = u_{fs}/2 \quad . \tag{2.21}$$

The free surface approximation of the particle velocity, $(u_{fs}/2)$, will usually exceed the particle velocity, u, by less than 0.5% due to the thermal expansion resulting from irreversible heating, except when melting occurs.[18,19]

Among the free surface measurement techniques[20] are shorting pins, capacitor microphone, slanted resistance wire, impedance match, high-speed photography and the interferometric techniques. Direct contact pressure transducers of materials which have pressure dependent electrical properties such as charge generation and resistance can be used. These transducers create an interface of two different materials; thus, the pressure-particle velocity Hugoniot of the material must be known as well as the pressure-electrical property change relation. The quartz[21] and manganin[22] gages are examples of interface transducers.

---

[18] Rice, McQueen and Walsh, "Compression of Solids ..."

[19] J. M. Walsh and R. H. Christian, Equation of State of Metals From Shock Wave Measurements, Phys. Rev., 97 (1955), 1544.

[20] D. G. Doran, Measurement of Shock Pressures in Solids. Poulter Laboratories TR 002-63 (April 1963).

[21] R. A. Graham, F. W. Neilson and W. B. Benedick, Piezoelectric Current from a Submicrosecond Stress Gage, J. Appl. Phys., 36 (1965), 1775-83.

[22] O. E. Williams, An Etched Manganin Gage System for Shock Pressure Measurement in a High Noise Environment. ISA Preprint Number P7-2-PHYMMID-67 (Sept. 1967).

The interferometric[23] technique is the best technique in terms of resolution, accuracy and frequency response and provides a free surface velocity history of both the loading and unloading behavior. Additional information about the material's shock behavior can be extracted from the free surface velocity history.

Shock wave data on materials are available and the principal reference is the Compendium of Shock Wave Data.[24] Principal sources of the data are the Los Alamos Scientific Laboratory, Lawrence Radiation Laboratory and Stanford Research Institute's Poulter Laboratories. Considerable data are available from the United Kingdom (Atomic Weapons Research Establishment) and Russian investigators such as Al'tshuler. The value of such data is dependent on the experimental technique and the abilities, experimental and theoretical, of the particular investigator.

The Mie-Grüneisen equation of state[25,26,27] is used extensively in interpreting shock wave data and is based on partition of the specific internal energy into two components.

$$E = E_V\left(v\right) + E_T\left(v,T\right) \qquad (2.22)$$

---

[23] L. M. Barker, Fine Structure of Compressive and Release Wave Shapes in Aluminum Measured by the Velocity Interferometer Technique, Proceedings of the IUTAM Conference on High Dynamic Pressures, Paris, France, September 1967, (1968), 483-505.

[24] Van Thiel, et al., Compendium of Shock Wave Data. University of California Lawrence Radiation Laboratory, Vol. 1 and II, June 1966.

[25] Rice, McQueen and Walsh, "Compression of Solids ..."

[26] Slater, "Introduction of Chemical ..."

[27] Born and Huang, "Dynamic Theory of ..."

The first component is volume dependent and is the lattice potential energy and the second component is the thermal lattice vibrational energy. Separation of the pressure associated with a particular volume-specific internal energy state into lattice and thermal pressure components, P_V and P_T, results in the Mie-Grüneisen equation[28]

$$P - P_V = \left(\gamma/v\right)\left(E - E_V\right) \tag{2.23}$$

where γ is the Grüneisen ratio defined by equation (2.20). Useful alternate definitions of the Grüneisen ratio are

$$\begin{aligned}\gamma &\equiv \beta B_T/\left(\rho C_V\right) \equiv v\left(\partial P/\partial E\right)_V \equiv -\left(v/C_V\right)\left(\partial P/\partial v\right)_T\left(\partial v/\partial T\right)_P \\ &\equiv -\left(v/C_P\right)\left(\partial P/\partial v\right)_S\left(\partial v/\partial T\right)_P\end{aligned} \tag{2.24}$$

The thermal coefficient of volume expansion, the isothermal bulk modulus and the specific heats at constant volume and constant pressure are β, B_T, C_V and C_P. A general form is obtained by considering any known thermodynamic path for the reference path states (P_R, E_R); then

$$P - P_R\left(v\right) = \left(\gamma/v\right)\left[E - E_R\left(v\right)\right] \quad . \tag{2.25}$$

When the Hugoniot is used as the reference path, comparisons in terms of pressure or energy offsets can be made with other thermodynamic processes.[29]

Experimental evaluation of a material's shock behavior in a series of shock wave experiments is a difficult, time consuming and costly process. Isothermal equations of state, theoretical and

---

[28] Rice, McQueen, and Walsh, "Compression of Solids ..."

[29] A. L. Ruoff, Linear Shock-Velocity-Particle-Velocity Relationship, J. Appl. Phys., 38 (1967), 4976.

empirical, have been developed to describe material behavior. Some of the equations developed by different investigators are

$$P = \left[B_{TO}/\left(1 + B'_{TO}\right)\right]\left\{1 - \left[1 - \left(1 + B'_{TO}\right)\left(v_o - v\right)/\left(2v_o\right)\right]^{1/2}\right\} \quad (2.26)$$

(Bridgman[30])

$$P = \left(B_{TO}/B'_{TO}\right)\left[\left(v_o/v\right)^{B'_{TO}} - 1\right] \quad \text{(Murnaghan[31])} \quad (2.27)$$

$$P = \left(3B_{TO}/2\right)\left[\left(v_o/v\right)^{7/3} - \left(v_o/v\right)^{5/3}\right] \quad \text{(Birch[32])} \quad (2.28)$$

$$P = \left[B_{TO}/\left(3 + B'_{TO}\right)\right]\left(v_o/v\right)^{2/3}$$

$$\left\{e \exp - 3\left(3 + B'_{TO}\right)\left[1 - \left(v_o/v\right)^{1/3}\right] - 1\right\} \quad (2.29)$$

(Pack-Evans-James[33])

In the equations (2.26), (2.27), (2.28) and (2.29), the constant coefficients are defined in terms of the isothermal bulk modulus and the pressure derivative of the bulk modulus, B_{TO} and B'_{TO}. The isothermal and adiabatic bulk moduli are related in the following fashion[34]

$$B_{TO} = B_{SO}/\left(1 + T\beta_o^2 B_{SO}/\rho C_p\right) \quad (2.30)$$

---

[30] Bridgman, "The Physics of ..."

[31] F. D. Murnaghan, The Compressibility of Media under Extreme Pressures, Proc. Natn. Acad. Sci., 30 (1944), 244.

[32] F. J. Birch, The Effect of Pressure Upon the Elastic Parameters of Isotropic Solids, According to Murnaghan's Theory of Finite Strain, J. Appl. Phys., 9 (1938), 279.

[33] D. C. Pack, W. M. Evans, and H. J. James, The Propagation of Shock Waves in Steel and Lead, Proc. Phys. Soc., 60 (1948), Part I.

[34] Overton, "Relation Between Ultrasonically ..."

where

$$B_{TO} = - v(0)\left(\partial P/\partial v(0)\right)_T \tag{2.31}$$

$$B_{SO} = - v(0)\left(\partial P/\partial v(0)\right)_S \tag{2.32}$$

$$\beta_O = \left(1/v(0)\right)\left(\partial v(0)/\partial T\right)_P \tag{2.33}$$

and

$$B'_{TO} = \left(\partial B_{SO}/\partial P\right)_T + \left(Tv(0)\beta_O^2 B_{TO}/C_P\right) \left[1 - 2\left(\partial B_{TO}/\partial T\right)_P/\beta_O B_{TO} - 2\left(\partial B_{SO}/\partial P\right)_T\right] + \left[Tv(0)\beta_O^2 B_{TO}/C_P\right]^2\left[\left(\partial B_{SO}/\partial P\right)_T - 1 - \left(\partial \beta_O/\partial T\right)_P/\beta_O^2\right] . \tag{2.34}$$

Values of the adiabatic bulk modulus and its derivates, B_{SO}, $\left(\partial B_{SO}/\partial P\right)_T$ and $\left(\partial B_{SO}/\partial T\right)_P$, can be determined from ultrasonic measurements[35,36] and combined with thermophysical property data in equations (2.30) and (2.34) to evaluate the isothermal bulk modulus and its pressure derivative. If experimental isothermal pressure-volume data are available, the constant coefficients of the different equations of state can be evaluated directly. The Bridgman equation is an empirical form resulting from experimental observation. The *Murnaghan* equation is based on the assumption that the bulk modulus increased linearly with pressure. A three-term strain-energy expansion in powers of linear strain and an assumed isothermal bulk modulus derivative value of four determines the Birch equation. The Pack-Evans-James

---

[35] D. Lazarus, The Variation of the Adiabatic Elastic Constant of KCl, NaCl, CuZn, Cu, and AL with Pressure to 10,000 Bars, Phys. Rev., 76 (1949), 545.

[36] H. J. McSkimin and P. Andreatch, Jr., Analysis of the Pulse Superposition Method of Measuring Ultrasonic Wave Velocities as a Function of Temperature and Pressure, J. Acoust. Soc. Am., 34(1962),609.

equation is an exponential form based on the Fermi-Thomas model of the atom.

An extension of a crystalline solid atomic model[37]

$$E = - a r^{-m} + b r^{-n}, \quad m > n, \tag{2.35}$$

was used by Fürth[38] to obtain the equation of state

$$P = \left(1/v\right) \left[\Lambda H \left(\xi\right) + R T G\left(\xi\right) \right] \tag{2.36}$$

where

$$H\left(\xi\right) = \left(m n \xi/3 \bar{S}\right) \left(1 + \xi\right)^{m/\bar{s}} \tag{2.37}$$

$$1 + \xi = \left(v/\bar{v}_0 \right)^{\bar{S}/3} . \tag{2.38}$$

$$G\left(\xi\right) = c + b \left[\left(1 + \xi\right)/\left(1 + K\xi\right) \right] \tag{2.39}$$

$$b = K\bar{S}/2 \tag{2.40}$$

$$c = 1 + m/2 \tag{2.41}$$

$$K = \left[1 - \left(m - 1\right) \int_n^\infty \int_{m+2}^\infty / \, n - 1 \int_m^\infty \int_{n+2}^\infty \right]^{-1} \tag{2.42}$$

$$\bar{S} = n - m \tag{2.43}$$

$$1 + \xi_0 = \left(\bar{v}_0/v_0 \right)^{\bar{S}/3} . \tag{2.44}$$

The specific volume v in cm^3/mole at pressure P and temperature T, the specific volume $\bar{v}_0$ at P = T = 0, the specific volume v_0 at room temperature and zero pressure, the heat of sublimation Λ in k cal/mole, the gas constant R in k cal/mole degree, the exponents m and n, and

---

[37] M. Bradburn, The Equation of State for a Face-Centered Cubic Lattice., Proc. Camb. Phil. Soc., 39 (1943), 113.

[38] R. Fürth, On the Equation of State for Solids, Proc. Roy. Soc., A183 (1944), 87.

the lattice sums $\left\{ \int_p^o \right\}$ tabulated by Misra[39] define the parameters of the equation.

The equations of state by Bridgman, Murnaghan, Birch, Pack-Evans-James and Fürth have been successfully applied to metallic solids and geological materials. These equations are applicable to polymeric solids even though the polymeric structure is not crystalline and the volume changes are more sensitive to pressure and temperature variation, however, care must be exercised. A generalized pressure-volume-temperature equation of state,

$$v = \left(0.01205/\rho_o^{0.9421}\right) P^{\bar{n}-1} \left(T/T_g\right)^{\bar{m}+2} + R \qquad (2.45)$$

has been developed by Whitaker and Griskey.[40] The variables of the equation are the initial density ρ_o, the glass transition temperature T_g, the universal gas constant R, the pressure P and the two pressure dependent constants $\bar{m}$ and $\bar{n}$. Other equations of state have been developed by Spencer and Gilmore,[41] Flory et al,[42] and DiBenedetto.[43]

---

[39] R. D. Misra, On the Stability of Crystal Lattices. II, Proc. Camb. Phil. Soc., 36 (1940), 175.

[40] H. L. Whitaker and R. G. Griskey, A Generalized Equation of State for Polymers, J. Appl. Polymer Sci., 11 (1967), 1001-8.

[41] R. S. Spencer and G. P. Gilmore, Equation of State for Polystyrene, J. Appl. Phys., 20 (1949), 504.

[42] P. J. Flory, R. A. Orwall, and A. Vrijo, Statistical Thermodynamics of Chain Molecule Liquids - I. An Equation of State for Normal Paraffin Hydrocarbons, J. Am. Chem. Soc., 86 (1964), 3507.

[43] A. T. DiBenedetto, Molecular Properties of Amorphous High Polymers - I. A Cell Theory for Amorphous High Polymers, J. Polymer Sci. A., 1 (1963), 3459.

Duvall[44,45] has shown that the isothermal state path can be transformed to the Hugoniot path if the specific heat at constant volume is independent of temperature and the specific internal energy is portioned into distortional and thermal vibrational components. The energy partition is based on Born's[46] model of a crystalline solid and permits a similar separation of the pressure components such that

$$P\left(v,T\right) = V_1\left(v\right) + T\, V_2\left(v\right) . \tag{2.46}$$

When the isothermal and Hugoniot pressures, P_i and P_h, that can be reached from an initial state (P_o, v_o, T_o) are expressed by

$$P_i\left(v\right) = V_1\left(v\right) + T_o V_2\left(v\right) \tag{2.46a}$$

$$P_h\left(v\right) = V_1\left(v\right) + T_h V_2\left(v\right) \tag{2.46b}$$

the equating of the two alternate energy expressions gives

$$E_h - E_o = C_v\left(T_h - T_o\right) + \int_{v_o}^{v} V_1\left(v\right) dv = \left(1/2\right)\left(P_h + P_o\right)\left(v_o - v\right) . \tag{2.47}$$

Substitution of the equivalent temperature difference, $\left[P_h\left(v\right) - P_i\left(v\right)\right]/V_2\left(v\right)$, that is obtained from equations (2.46a) and (2.46b), in equation (2.47) and rearranging terms yields

$$P_h\left(v\right) = \left[P_i\left(v\right) - \left(V_2\left(v\right)/C_v\right)\int_{v_o}^{v} V_1\left(v\right)dv\right]/\left[1 - \left(V_2\left(v\right)/2C_v\right)\left(v_o - v\right)\right] . \tag{2.48}$$

---

[44] Duvall and Zwolinski, "Entropic Equations of ..."

[45] Duvall, "Pressure-Volume Relations ..."

[46] Born and Huang, "Dynamic Theory of ..."

Figure 2.5 illustrates the path prescribed by equation (2.48) to arrive at the Hugoniot pressure P_h.

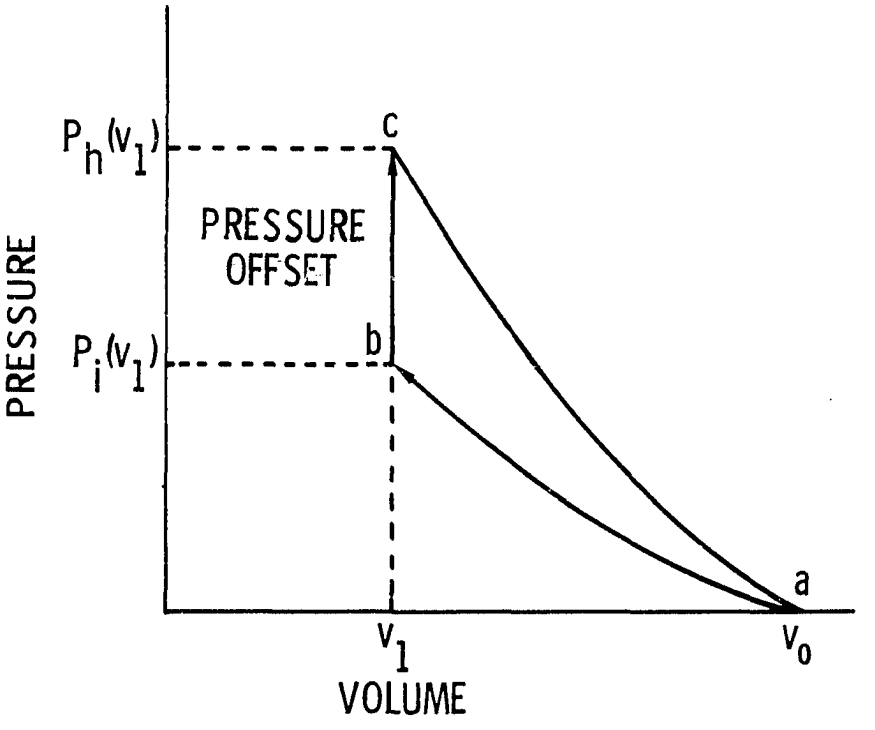

Figure 2.5 Pressure Offset Between Isothermal and Hugoniot States

The isothermal pressure $P_i(v)$ can be obtained from any of the previous equations of state, equations (2.26), (2.27), (2.28) and (2.36), and the remaining pressure increment, $P_h(v) - P_i(v)$, is the result of an increase in temperature from T_0 to T_h at a constant volume value of v_1; therefore,

$$P_h\left(v\right) = P_i\left(v\right) + \left[\left(T/v\right) - \left(T_0/v_0\right)\right]\beta B_{T0}\, v_0 \qquad (2.49)$$

Then the first and second volume functions, $V_1(v)$ and $V_2(v)$ are

$$V_1\left(v\right) = P_i\left(v\right) - T_0\beta B_{T0} \qquad (2.50)$$

$$V_2\left(v\right) = \beta B_{T0} v_0/v \quad . \qquad (2.51)$$

An alternate method of evaluating the pressure offsets between the Hugoniot and isothermal paths utilizes the Mie-Grüneisen equation with the Hugoniot as the reference such that

$$P_h(v) = \left[P_i(v) + (\gamma/v)\int_{V_0}^{V} P(v)dv\right] / \left[1 - \right.$$

$$\left. - (\gamma/v)(v_0 - v)/2\right] . \qquad (2.52)$$

The experimental techniques for isothermal pressure-volume measurements have been documented by Bridgman and others. A high-pressure cell containing the test specimen is subjected to high fluid pressure with a fluid and the pressures and the accompanying specimen volume changes are measured carefully. Another technique used by Stevens utilized a zero-clearance constraint cylinder about the test specimen which was loaded by close-fitting guided rams. Measurements were made of ram force and relative displacement of the loading rams to obtain the specimen pressure and volume. Both methods are pressure limited (< 30 kbar). The pressure cell method does not subject the specimen to the friction forces which are present in the laterally confined specimen test method. Appreciable stress and strain gradients in the laterally confined specimen are due to the friction forces. Stevens compensated for the friction effects by using a correction factor obtained from the compression of a known material, gold. Both methods are limited in pressure (< 30 kbar) but do not require a substantial amount of raw material for the specimen. The laterally confined compression method is simpler and less expensive than the high-pressure cell technique.

The ultrasonically determined isothermal bulk modulus and the pressure derivative of the isothermal bulk modulus, B_{TO} and B'_{TO}, can be used to evaluate the constant coefficients of the various isothermal equations of state (see equations (2.26), (2.27), (2.28) and (2.29)). This indirect method is detailed by Overton and Anderson and a good description of the experimental techniques used to evaluate the bulk modulus and its pressure derivative is described by McSkimin.[47] Ultrasonic test equipment, an environmental test cell with temperature and pressure variation capabilities and considerable ability in interpreting ultrasonic records is needed to make the necessary measurements.

Isothermal equations of state have been determined by direct measurement[48,49,50] and the indirect ultrasonic method[51,52,53,54] for a number of metals and some non-metallic materials. Evaluation of the isothermal equation of state of low strength single-phase polymers by

---

[47] McSkimin and Andreatch, "Analysis of the ..."

[48] Bridgman, "The Physics of ..."

[49] R. W. Warfield, Compressibility of Bulk Polymers, Poly. Engr. and Sci., 6 (1966), 176-80.

[50] R. W. Warfield, The Compressibility of Polymers to 20000 Atmospheres, Naval Ordnance Laboratory NOLTR-66-45 (June 1966).

[51] Overton, "Relation Between Ultrasonically ..."

[52] Anderson, "The Use of ..."

[53] Ruoff, "Linear Shock-Velocity ..."

[54] C. A. Rotter and C. S. Smith, Ultrasonic Equation of State of Iron - I. Low Pressure, Room Temperature, J. Phys. Chem. Solids, 27 (1966), 267-76.

the direct pressure-volume measurement methods and the indirect ultrasonic technique, appears to be feasible. The overall simplicity of the laterally confined compression method has considerable appeal.

CHAPTER III

THE MURNAGHAN FORM AND TRANSFORMATIONS

The Murnaghan equation of state[55] is based on the assumption that the isothermal bulk modulus of a material increases linearly with pressure, i.e.

$$B_T = - v(\partial P/\partial v)_T = B_{TO} + B'_{TO}P \quad . \tag{3.1}$$

Integration of the linear pressure vs. bulk modulus relation gives

$$\ell n\ (v_O/v) = (1/B'_{TO})\ \ell n \left[B'_{TO}\,(P/B_{TO}) + 1 \right] \tag{3.2}$$

which can be manipulated to yield the standard Murnaghan form

$$P = (B_{TO}/B'_{TO}) \left[(v_O/v)^{B'_{TO}} - 1 \right] . \tag{3.3}$$

A more general expression is a MacLaurin series expansion in terms of pressure so that

$$B = B_O + B'_O\, P + (1/2)\, B''_O\, P^2 + (1/6)\, B'''_O\, P^3 + (1/24)\, B''''_O\, P^4 + \ldots \tag{3.4}$$

where the primes represent differentiation with respect to pressure and the bulk modulus, B, can be either the isothermal value B_T or the adiabatic value B_S. The relationship between the isothermal and the adiabatic bulk moduli and their pressure derivatives can be obtained from the established thermodynamic formulas

---

[55] Murnaghan, "The Compressibility of Media . . . ."

$$C_P - C_V = T\, v\, \beta^2 B_T \quad . \tag{3.5}$$

$$(1/B_T) - (1/B_S) = T\, v\, \beta^2/C_P \quad . \tag{3.6}$$

The thermodynamic variables, C_V the specific heat at constant volume, C_P the specific heat at constant pressure, β the thermal coefficient of volume expansion, B_T the isothermal bulk modulus, and B_S the adiabatic bulk modulus, have the following thermodynamic definitions

$$C_P = (\partial E/\partial T)_P \tag{3.7a}$$

$$C_V = (\partial E/\partial T)_V \tag{3.7b}$$

$$\beta = (1/v)(\partial v/\partial T)_P \tag{3.7c}$$

$$B_T = - v(\partial P/\partial v)_T \tag{3.7d}$$

$$B_S = - v(\partial P/\partial v)_S \tag{3.7e}$$

Equation (3.6) identifies the isothermal bulk modulus as

$$B_T = B_S(C_V/C_P) = B_S/(1 + T\, v\, \beta^2 B_S/C_P) \quad . \tag{3.8}$$

The isothermal bulk modulus pressure derivative is

$$B_T' = B_S' + (T\, v\, \beta^2 B_T/C_P)\left[1 - 2(\partial B_T/\partial T)_P/\beta B_T - 2(\partial B_S/\partial P)_T\right]$$

$$+ (T\, v\, \beta^2 B_T/C_P)^2\left[(\partial B_S/\partial P)_T - 1 (\partial \beta/\partial T)_P/\beta^2\right] \quad . \tag{3.9}$$

The role of the bulk modulus and its pressure derivatives in the isothermal equation of state can be seen when the pressure derivatives of the volume are evaluated for the following general MacLaurin series representation of an isothermal equation of state

$$v(P) = v(0) + v'(0)P + (1/2)\, v''(0)P^2 + (1/6)\, v'''(0)P^3$$

$$+ (1/24)\, v''''(0)P^4 + \ldots . \tag{3.10}$$

Rearranging equation (3.7d), the thermodynamic definition of the isothermal bulk modulus, to obtain

$$v'(0) = - v(0)/B_{TO} \tag{3.11}$$

and evaluating the next three pressure derivatives of the initial

volume gives

$$v''(0) = \left(v(0)/B_{TO}^2\right)\left(1 + B_{TO}'\right) = v(0)m/B_{TO}' \tag{3.12}$$

$$v'''(0) = \left(v(0)/B_{TO}^3\right)\left[1 + 3B_{TO}' + 2(B_{TO}')^2 - B_{TO}B_{TO}''\right] = -v(0)n/B_{TO}^3 \tag{3.13}$$

$$v''''(0) = \left(v(0)/B_{TO}^4\right)\left[1 + 6B_{TO}' + 11(B_{TO}')^2 - 4B_{TO}B_{TO}'' + 6(B_{TO}')^3 - 6B_{TO}B_{TO}'B_{TO}'' + B_{TO}^2B_{TO}'''\right] = v(0)q/B_{TO}^4 \quad . \tag{3.14}$$

Now the first five terms of equation (3.10) can be expressed as

$$v(P) = v(0)\left(1 - 1/B_{TO} + m/B_{TO}^2 - n/B_{TO}^3 + q/B_{TO}^4 + \ldots\right) \tag{3.15}$$

The Murnaghan equation can be transformed from the isothermal form (equation (3.3)) to obtain the isentrope and Hugoniot pressures by a method described by Duvall.[56,57] The method is based on partitioning the specific internal energy into distortional and thermal vibrational components such that the pressure is related to the volume and the temperature in the following fashion

$$P = V_1(v) + TV_2(v) \quad . \tag{3.16}$$

Figure 3.1 illustrates the isothermal, isentropic and Hugoniot paths. Duvall evaluated the isentrope and Hugoniot in terms of the isothermal pressure and the corresponding constant-volume pressure offset to the isentrope and Hugoniot.

---

[56] Duvall and Zwolinski, "Entropic Equations of State . . . ."

[57] Duvall, "Pressure-Volume Relations . . . ."

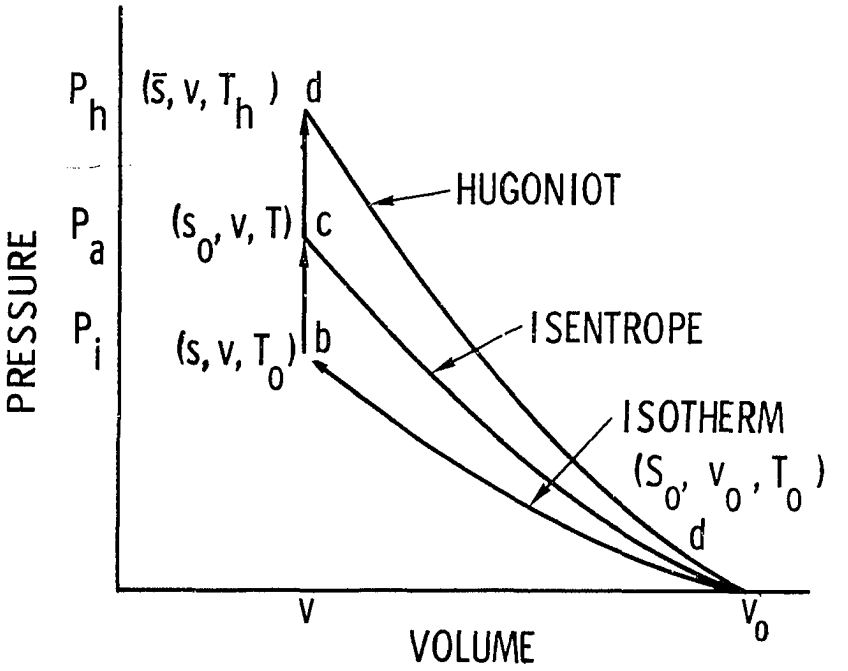

Figure 3.1 Pressure Offsets Between the Isotherm, Isentrope and Hugoniot States

Expressing the Murnaghan equation in the form of equation (3.16) gives

$$P = (B_{TO}/B'_{TO})\left[(v_0/v)^{B'_{TO}} - 1\right] + \left[(T/v) - (T_0/v_0)\right] 3B_{TO}v_0 \quad (3.17)$$

such that the functions $v_1(v)$ and $v_2(v)$ are

$$V_1(v) = (B_{TO}/B'_{TO})\left[(v_0/v)^{B'_{TO}} - 1\right] - T_0 3B_{TO} \quad (3.18)$$

$$V_2(v) = 3B_{TO}v_0/v \quad . \quad (3.19)$$

The increase in entropy from point b on the isotherm to point c on the isentrope is

$$\int_{s}^{s_0} (1/C_v)dS = \int_{T_0}^{T} (1/T)dT \quad (3.20)$$

if the specific heat of constant volume, C_v, is independent of entropy. By using the Maxwell relation,

$$(\partial S/\partial v)_T = (\partial P/\partial T)_v \quad , \quad (3.21)$$

the change in entropy from point a to point b along the isotherm can be identified as

$$\int_{S_o}^{S}(1/C_v)dS = \int_{V_o}^{V}(\partial S/\partial v)\,(1/C_v)dv = \int_{V_o}^{V}(\partial P/\partial T)_{v@T_o}\,(1/C_v)dv \qquad (3.22)$$

Substituting the derivative of the pressure with respect to temperature at constant volume that is obtained by differentiating equation (3.17), into equation (3.22) permits equation (3.20) to be written as

$$\int_{S}^{S_o}(1/C_v)dS = \int_{T_o}^{T}(1/T)dT = -\int_{V_o}^{V} V_2(v)/C_v\ dV = \int_{V}^{V_o} V_2(v)/C_v\ dV \qquad (3.23)$$

Integration of equation yields

$$\ell n(T/T_o) = (\beta B_{To} v_o/C_v)\,\ell n(v_o/v) \quad . \qquad (3.24)$$

Equation (3.24) expressed in the desired alternate form gives the temperature at point c on the isentrope as

$$T = T_o \exp(\beta B_{To} v_o/C_v) \quad . \qquad (3.25)$$

Substituting equation (3.25) for the temperature T, in equation (3.17) defines the pressure, P_a, on the isentrope at point c as

$$P_a = B_{To}/B'_{To}\left[(v_o/v)^{B'_{To}} - 1\right] + T_o\beta B_{To}\left[(v_o/v)^{(1+\beta B_{To}v_o/C_v)} - 1\right] \qquad (3.26)$$

Transformation from point b on the isothermal path to point d on the Hugoniot utilizes the Rankine-Hugoniot energy conservation equation,

$$E_h - E_o = (1/2)\,(P_h + P_o)(v_o - v) \quad , \qquad (3.27)$$

and the equivalent energy expression

$$E_h - E_o = \int_{V_o}^{V} V_1(v)dv + C_v\,(T_h - T_o) \quad . \qquad (3.28)$$

The temperature difference, $T_h - T_o$, is obtained from the following equations

$$P_i = V_1(v) + T_o V_2(v) \quad . \qquad (3.29)$$

$$P_h = V_1(v) + T_h V_2(v) \quad . \qquad (3.30)$$

such that

$$\int_{S_o}^{S}(1/C_v)dS = \int_{V_o}^{V}(\partial S/\partial v)\,(1/C_v)dv = \int_{V_o}^{V}(\partial P/\partial T)_{v@T_O}\,(1/C_v)dv \qquad (3.22)$$

Substituting the derivative of the pressure with respect to temperature at constant volume that is obtained by differentiating equation (3.17), into equation (3.22) permits equation (3.20) to be written as

$$\int_{S}^{S_o}(1/C_v)dS = \int_{T_o}^{T}(1/T)dT = -\int_{V_o}^{V} V_2(v)/C_v\ dV = \int_{V}^{V_o} V_2(v)/C_v\ dV \qquad (3.23)$$

Integration of equation yields

$$\ell n(T/T_o) = (\beta B_{TO} v_o/C_v)\,\ell n(v_o/v) \quad . \qquad (3.24)$$

Equation (3.24) expressed in the desired alternate form gives the temperature at point c on the isentrope as

$$T = T_o \exp(\beta B_{TO} v_o/C_v) \quad . \qquad (3.25)$$

Substituting equation (3.25) for the temperature T, in equation (3.17) defines the pressure, P_a, on the isentrope at point c as

$$P_a = B_{TO}/B'_{TO}\left[(v_o/v)^{B'_{TO}} - 1\right] + T_o\beta B_{TO}\left[(v_o/v)^{(1+\beta B_{TO}v_o/C_v)} - 1\right] \qquad (3.26)$$

Transformation from point b on the isothermal path to point d on the Hugoniot utilizes the Rankine-Hugoniot energy conservation equation,

$$E_h - E_o = (1/2)\,(P_h + P_o)(v_o - v) \quad , \qquad (3.27)$$

and the equivalent energy expression

$$E_h - E_o = \int_{V_o}^{V} V_1(v)dv + C_v\,(T_h - T_o) \quad . \qquad (3.28)$$

The temperature difference, $T_h - T_o$, is obtained from the following equations

$$P_i = V_1(v) + T_o V_2(v) \quad . \qquad (3.29)$$

$$P_h = V_1(v) + T_h V_2(v) \quad . \qquad (3.30)$$

such that

$$T_h = T_o = (P_h - P_i)/V_2(v) \quad . \tag{3.31}$$

Substituting equation (3.31) in equation (3.28) and equating the two energy expressions gives

$$(1/2)(P_h + P_o)(v_o - v) = \int_{v_o}^{v} V_1(v)dv + C_v \left[(P_h - P_i)/V_2(v) \right] \tag{3.32}$$

which can be arranged to obtain

$$P_h = \left[P_i - (V_2(v)/C_v) \int_{v_o}^{v} V_1(v)dv \right] \Big/ \left[1 - V_2(v)(v_o - v)/2C_v \right] . \tag{3.33}$$

Replacing the functions $V_1(v)$ and $V_2(v)$ with the equivalent Murnaghan values, equations (3.18) and (3.19) and integrating yields

$$P_h = P_i + (V_2(v)/C_v) \left\{ (P_i v_o/2 \left[1 - (v/v_o) \right] - V \right\} \Big/ \left\{ 1 - (V_2(v)v_o/2C_v) \left[1 - (v/v_o) \right] \right\} \quad . \tag{3.34}$$

where P_i and V are

$$P_i = (B_{TO}/B'_{TO}) \left[(v_o/v)^{B'_{TO}} - 1 \right] - T_o \delta B_{TO} \left[1 - (v_o/v) \right] \tag{3.35}$$

$$V = \left[B_{TO} v_o / B'_{TO} \left(B'_{TO} - 1 \right) \right] \left[(v_o/v)^{(B'_{TO} - 1)} - 1 \right] - \left(B_{TO}/B'_{TO} + \delta B_{TO} T_o \right) \left[1 - (v/v_o) \right] v_o \quad . \tag{3.36}$$

When the value of the adiabatic bulk modulus in the thermodynamic definition of the bulk modulus is replaced by a MacLaurin series expansion, the resulting differential equation is

$$- v \, (dP/dv)_s = B_{SO} + B'_{SO} \, P + (1/2) \, B''_{SO} \, P^2 + \ldots \quad . \tag{3.37}$$

Integration of equation (3.37) leads to the isentropic equation of state[58]

$$P = \left[(v/v_o)^{a_o} - 1 \right] \Big/ \left[a_1 - a_2 (v/v_o)^{a_1} \right] \tag{3.38}$$

where the constants a_0, a_1 and a_2 are

---

[58] Ruoff, "Linear Shock-Velocity . . . . "

$$a_o = \left[(B'_{To})^2 - 2B_{so}B''_{so}\right]^{1/2} \tag{3.38a}$$

$$a_1 = B''_{so}\Big/\left\{B'_{so} + \left[(B'_{so})^2 - 2B_{so}B''_{so}\right]^{1/2}\right\} = B''_{so}/(B'_{so} + a_o) \tag{3.38b}$$

$$a_2 = B''_{so}\Big/\left\{B'_{so} - \left[(B'_{so})^2 - 2B_{so}B''_{so}\right]^{1/2}\right\} = B''_{so}/(B'_{so} - a_o) \tag{3.38c}$$

By using the Mie-Grüneisen equation of state,

$$P_h - P = (\gamma/v)(E_h - E) \tag{3.39}$$

and the Hugoniot and isentrope energies,

$$E_h = (P_h + P_o)(v_o - v)/2 \tag{3.40}$$

$$E = -\int_{v_o}^{v} P\, d\, v \quad , \tag{3.41}$$

the Hugoniot pressure can be expressed as

$$P_h = \left[P + (\gamma/v)\int_{v_o}^{v} P\, d\, v\right] \Big/ \left[1 - (\gamma/v)(v_o - v)/2\right] \tag{3.42}$$

where the isentrope pressure, P, is obtained from equation (3.38) and the Grüneisen ratio is γ . When equation (3.42) is evaluated and combined with the first two Rankine-Hugoniot conservation equations,

$$v_o/v = U/(U - u) \tag{3.43}$$

$$P_h - P_o = U\, u/v_o \tag{3.44}$$

the coefficients of an assumed second-degree shock velocity-particle velocity relationship,

$$U = b_o + b_1 u + b_2 u^2 \tag{3.45}$$

can be expressed as

$$b_o = (B_{so} v_o)^{1/2} \tag{3.45a}$$

$$b_1 = (B'_{so} + 1)/4 \tag{3.45b}$$

$$\begin{aligned} b_2 &= \left\{\left[(B'_{so} + 1)/4\right](7 - B'_{so} + 4\gamma) + 2B_{so}B''_{so}\right\}\Big/24(B_{so}v_o)^{1/2} \\ &= \left[b_1(7 - B'_{so} + 4\gamma) + 2B_{so}B''_{so}\right]\Big/24b_o \end{aligned} \tag{3.45c}$$

The Grüneisen ratio, γ, is assumed to be a function of volume[59] of the form

$$\gamma = \gamma_0 + A_1\left[(v_0/v) - 1\right] + A_2\left[(v_0/v) - 1\right]^2 + \ldots \qquad (3.46)$$

Equation (3.46) can be expressed in an alternate form as

$$\gamma = \gamma_0 + A_1\left[u/(U - u)\right] + A_2\left[u/(U - u)\right]^2 + \ldots \qquad (3.47)$$

since

$$v_0/v - 1 = U/(U - u) - 1 = u/(U - u) \quad . \qquad (3.48)$$

The value of the second-degree coefficient, b_2, in equation (3.45) can now be written as

$$b_2 = \left[b_1(7 - B'_{s0} + 4\gamma_0) + 2B_{s0}B''_{s0}\right]/24b_0 \quad . \qquad (3.45d)$$

The isentropic equation of state, equation (3.38), obtained from equation (3.37), assumes that the adiabatic bulk modulus pressure derivatives beyond the second pressure derivative are negligibly small and the value of the constant, a_0, is positive definite. Ruoff[60] has found the effect of the second-degree term in the shock velocity-particle velocity relationship (equation (3.45)) as did Duvall[61] and Adler[62] in determining that the shock velocity-particle velocity relation of single-phase materials is linear.

Proceeding on the premise that the shock velocity-particle velocity relationship is linear, i.e.

---

[59] Rice, McQueen and Walsh, "Compression of Solids . . . ."

[60] Ruoff, "Linear Shock Velocity . . . . "

[61] Duvall and Fowles, "Shock Waves in High Pressure . . . ."

[62] B. J. Adler, Physics Experiments with Strong Pressure Pulses, in Solids Under Pressure. Edited by W. Paul and D. W. Warschauer. New York: Mc-Graw Hill, 1963.

$$U = b_0 + b_1 u = U_0 + b_1 u, \tag{3.49}$$

the Murnaghan equations of state for the isentrope and the Hugoniot in terms of an experimentally determined isothermal Murnaghan equation of state,

$$P = (B_{T0}/B'_{T0})\left[(v_0/v)^{B'_{T0}} - 1\right], \tag{3.3}$$

are

$$P = (B_{S0}/B'_{S0})\left[(v_0/v)^{B'_{S0}} - 1\right] \quad \text{(isentrope)} \tag{3.50}$$

where

$$B_{S0} = B_{T0}/(1 - B_{T0}T_0 v_0 \beta^2/C_P) \tag{3.50a}$$

$$B'_{S0} = B'_{T0} - (T_0 v_0 \beta^2 B_{T0}/C_P)\left[1 - (2/\beta B_{T0})(\partial B_{T0}/\partial T)_P - 2(\partial B_{S0}/\partial P)_T\right] + (T_0 v_0 \beta^2 B_{T0}/C_P)^2\left[(\partial B_{S0}/\partial P)_T - 1 - (1/\beta^2)(\partial \beta/\partial T)_P\right], \tag{3.50b}$$

and

$$P_h = P_i + (V_2(v)/C_V)\left\{(P_i/2)\left[1 - (v/v_0)\right]v_0 - V\right\}\Big/ \left\{1 - (V_2(v)/2C_V)\left[1 - (v/v_0)\right]v_0\right\} \quad \text{(Hugoniot)} \tag{3.34}$$

where

$$P_i = (B_{T0}/B'_{T0})\left[(v_0/v)^{B'_{T0}} - 1\right] - T_0 \beta B_{T0}\left[1 - (v_0/v)\right] \tag{3.35}$$

$$V = \left[B_{T0}v_0/B'_{T0}(B'_{T0} - 1)\right]\left[(v_0/v)^{B'_{T0}} - 1\right] - (B_{T0}/B'_{T0} + \beta B_{T0}T_0)\left[1 - (v/v_0)\right]v_0 . \tag{3.36}$$

CHAPTER IV

THE EXPERIMENTAL PROGRAM AND PROCEDURE

The experimental program was designed to investigate the role of specimen geometry and specimen-constraint cylinder friction in the laterally confined isothermal compression tests of low-strength polymers over a pressure range from 0 to 10 kbar. A series of laterally confined isothermal compression tests were run on six groups of polymethylmethacrylate (PMMA) specimens of different length-to-diameter ratios. The specimen deflection, the axial friction force between the specimen and the constraint cylinder wall, and the total load applied to the specimen were measured. A minimum of 15 specimens were tested in each of the six groups having length to diameter ratios of ℓ/d = 1/8, 1/4, 1/2, 1, 2, 4.

In addition to the constraint cylinder and the closely-fitting loading rams, a Baldwin subpress, a Kistler cylindrical load cell, a Baldwin deflectometer, a 30,000-pound capacity Tinius Olsen universal test machine, a Dymec digital data system, and force and deflection calibration equipment were used in the test setup. A detailed list of the commercial equipment that was used in the test program is presented in Table 4.1. Figure 4.1 shows the setup.

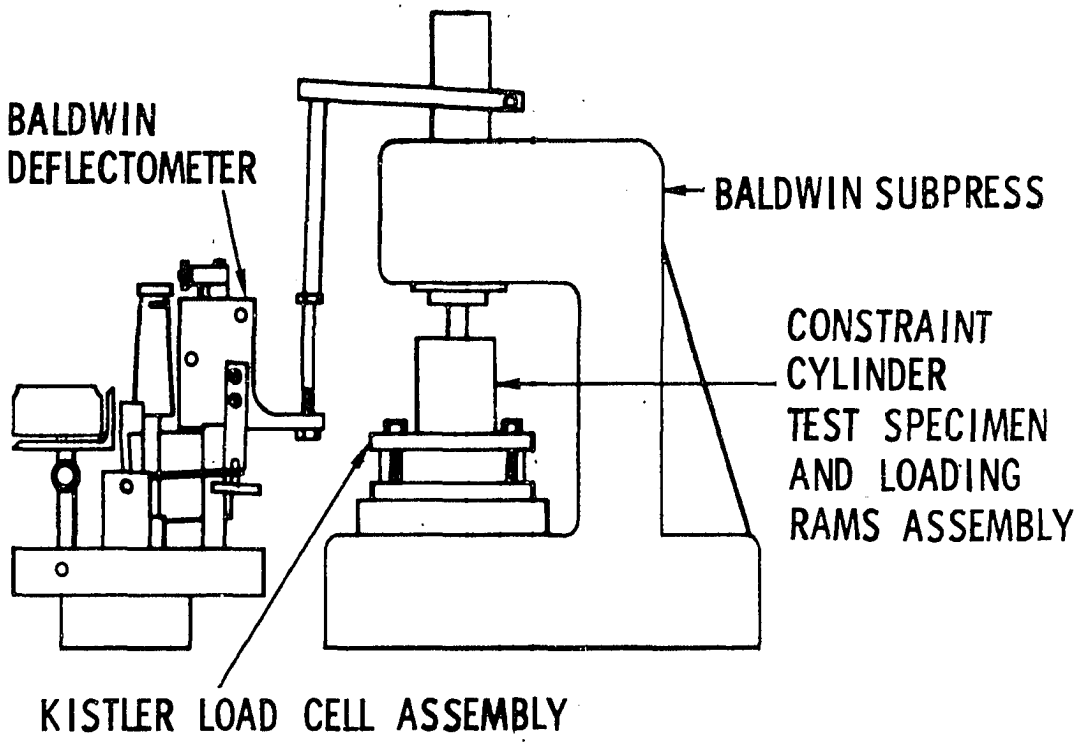

Figure 4.1 Test Set Up

The axial friction force was transferred from the base of the constraint cylinder to the bottom subpress platen by the cylindrical load cell and the force applied to the bottom loading ram by the specimen was transferred to the bottom subpress platen by the load button. (See Figure 4.2).

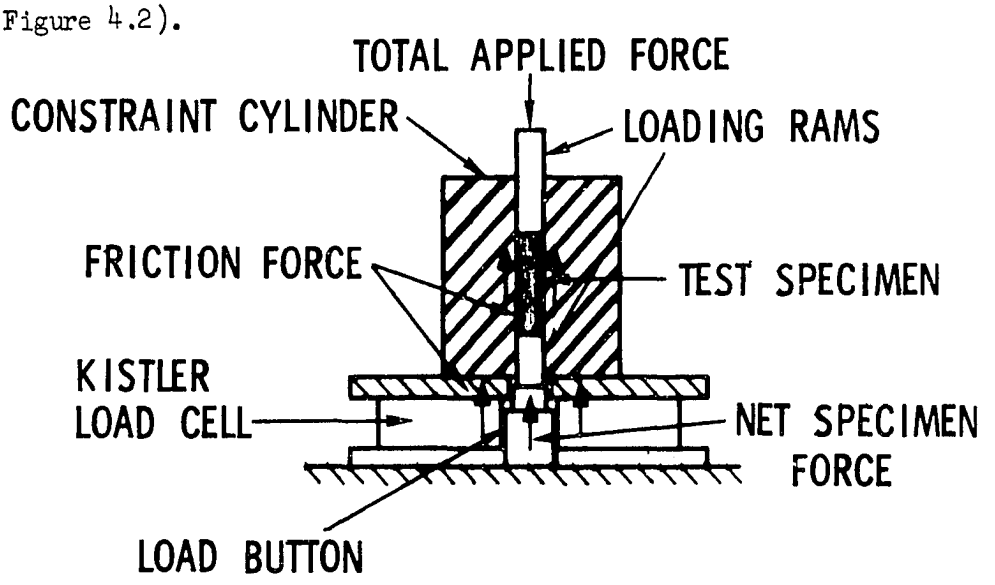

Figure 4.2 Test specimen-constraint cylinder-load cell assembly

The total force applied to the upper loading ram was measured with the testing machine's force measuring system and the axial friction force was measured with the cylindrical load cell. The test specimen deformation was determined by measuring the relative displacement of the subpress platens with a deflectometer. A digital data system was used to record the relative platen displacement, axial friction force, and the total applied force. The deflectometer was calibrated before and after testing each group of specimens with an Instron extensiometer calibrator. Doall gage blocks were used to check the calibration before each test. Since both force measuring systems, the cylindrical load cell and the testing machine's force measuring system, could be electronically stepped to cover different force ranges, calibration of the force measuring systems was carried out in 15-pound load increments over the 150-pound force range with Instron calibration weights. Calibration of the force and displacement measuring systems included the digital data system. The average overall errors of five calibration runs for the relative platen displacement, axial friction force and total applied force measuring systems were 0.52, 0.89 and 0.47 per cent, respectively. (See Table 4.2.)

The constraint cylinders and the loading rams were fabricated of 4340 steel heat treated to a hardness of 52 Rockwell C with ground surfaces. Two constraint cylinders, 2.000 and 4.000 inches in length, with outside and inside diameters of 2.000 and 0.5046 inches were used. The 0.5034 inch diameter of the two loading ram sets, 2.000 and 0.500 inches in length, was selected to provide minimum clearance under maximum load (150,000 pounds). Details of the constraint

cylinders and the loading rams are shown in Figure 4.3. The test specimen dimensions are detailed in Figure 4.4. Figure 4.5 shows the cylindrical load-cell fixture details.

The step-by-step test procedure that was used in the individual tests is:

1) carefully clean each of the specimens, constraint cylinder, and loading rams with alcohol.
2) measure and record the diameter and length of the specimen.
3) coat the specimen, loading rams and the internal diameter of the constraint cylinder with a molybdenum disulfide solution and let the parts dry.
4) cool the test specimen to 50°F.
5) assemble the test specimen, constraint cylinder, and loading rams, place the assembly in the subpress; and properly position the assembly on the cylindrical load cell with the bottom loading ram in contact with the load button.
6) wait until thermal equilibrium is achieved (approximately 15 minutes); then check the loading ram and reposition to remove any clearance between the bottom loading ram and the load button.
7) check the deflectometer calibration by placing a Doall gage block between the deflectometer-upper platen connection.
8) zero the force measuring systems.
9) start the testing machine's continuous force-deflection recorder.
10) begin loading the specimen at a rate of 0.010 inch per minute.

11) stop the testing machine and read with the digital data system the output of the deflectometer and the load cells as loading on the specimen begins and at each of ten load values; 3000 to 30,000 pounds in 3000 pound increments.

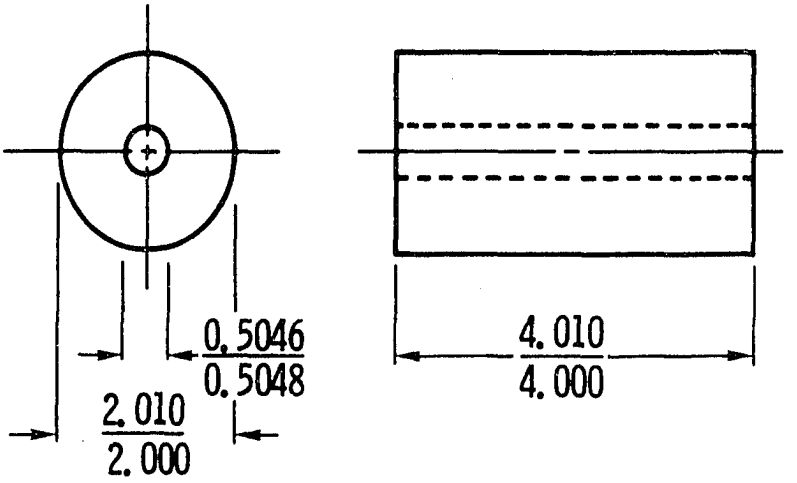

LONG CONSTRAINT CYLINDER

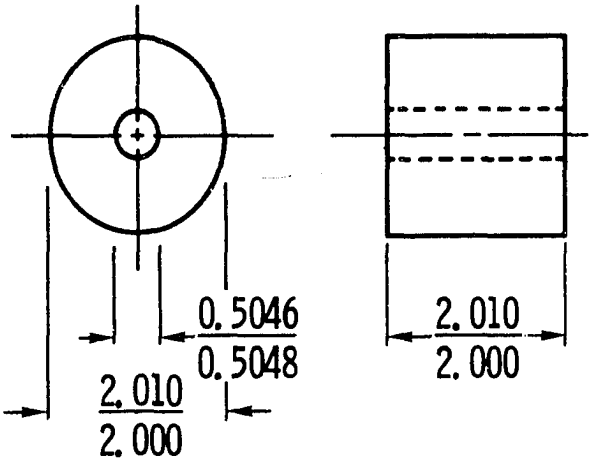

SHORT CONSTRAINT CYLINDER

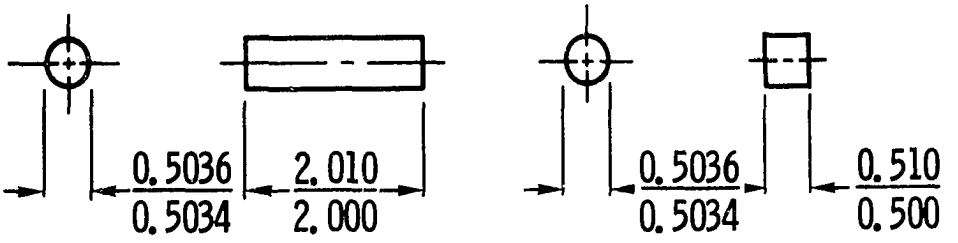

LONG LOADING RAM SHORT LOADING RAM

Notes: 1. Material 4340 heat treated to 52 R.C.

2. All surfaces $\sqrt{32}$ or better

3. Ends of cylinders and rams must be flat and parallel within .0005

4. All dimensions in inches

Figure 4.3 Constraint Cylinder and loading ram details

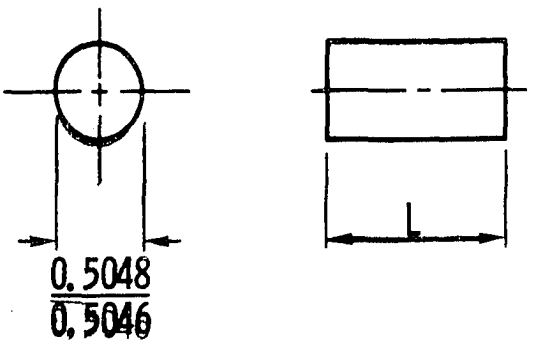

Notes:

1. Ends of cylinder must be flat and parallel within .0005
2. All surfaces $\sqrt{32}$ or better
3. All dimensions in inches

SPECIMEN SERIES	DIMENSIONS LENGTH, IN.
100	0.063 + 0.000 - 0.001
200	0.125 + 0.000 - 0.001
300	0.250 + 0.000 - 0.001
400	0.500 + 0.000 - 0.001
500	1.000 + 0.000 - 0.001
600	2.000 + 0.000 - 0.001

Figure 4.4 Test specimen dimensions

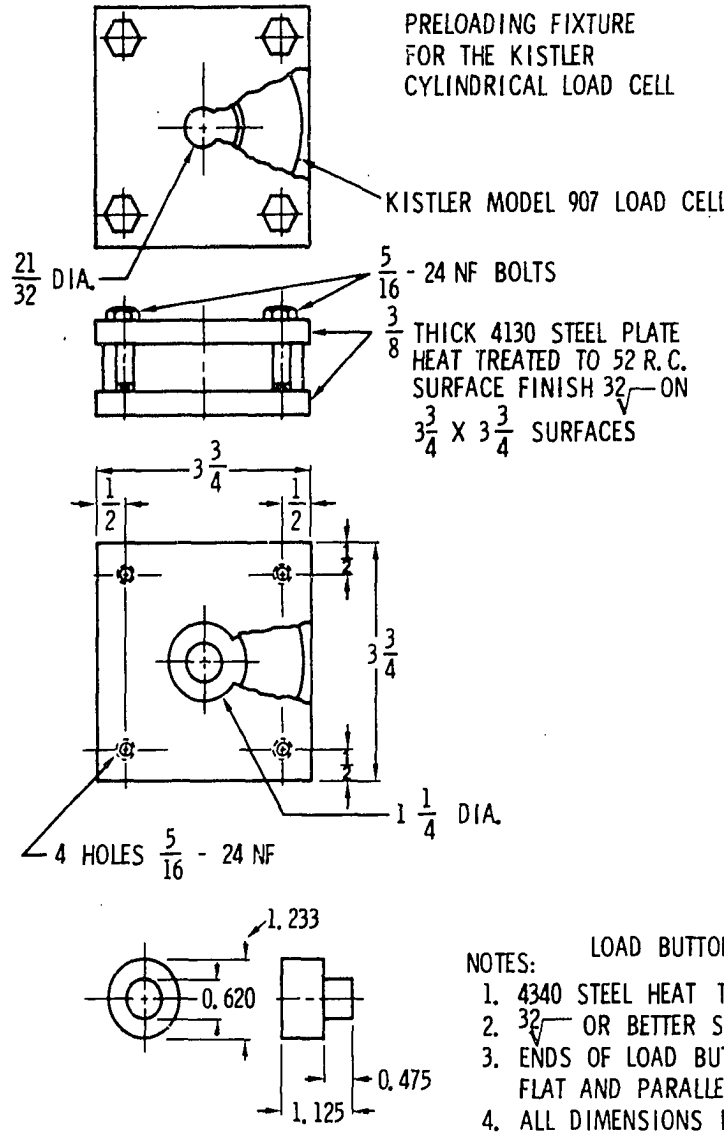

Figure 4.5 Load-Cell Fixture Details

TABLE 4.1

TABLE OF COMMERCIAL EQUIPMENT

1. 30,000 pound Tinius Olsen, Model X-Y 8, universal test machine.
2. Baldwin Model PDIM Multiple Range Deflectometer.
3. Doall Precision Gage Blocks, Set 35-S.
4. Instron Extensiometer Calibrator
5. Instron Class "C" Calibration Weights
6. Kistler Model 907 Load Cell, 60,000 pound capacity
7. Kistler Model 568 Charge Amplifier
8. Digital Data System
   a. Dymec Model 2401C Integrating Digital Voltmeter
   b. Hewlett-Packard J66 562a Digital Printer
   c. Dymec Model 2901A Input Scanner
9. Molybdenum lubricant number 369 dry lubricant manufactured by Imperial Oil and Grease Company.

TABLE 4.2

TEST SYSTEM CALIBRATION

Reading Number	Calibration Values, %: Displacement % of Total Output	Overall Force Reading, % of Total Output	Friction Force Reading, % of Total Output
1	10.526	10.000	10.000
2	21.053	20.000	20.000
3	31.579	30.000	30.000
4	42.105	40.000	40.000
5	52.632	50.000	50.000
6	63.158	60.000	60.000
7	73.684	70.000	70.000
8	84.211	80.000	80.000
9	94.737	90.000	90.000
10	100.000	100.000	100.000

Reading Number	Displacement Error, %	Overall Force Error, %	Friction Force Error, %
Run Number 1			
1	- 2.47	- 0.36	1.52
2	- 0.89	0.24	- 1.02
3	- 0.24	0.85	- 1.86
4	- 0.01	1.05	- 1.02
5	0.29	1.01	- 1.52
6	0.16	0.38	- 0.17
7	0.07	0.68	- 0.65
8	0.09	0.34	- 0.38
9	- 0.15	0.31	- 0.17
Average Error	0.48	0.58	0.92
Run Number 2			
1	- 2.71	- 0.08	- 1.48
2	- 1.12	0.93	0.99
3	- 0.46	0.59	0.16
4	0.26	0.63	- 0.25
5	0.38	0.97	0.49
6	0.33	0.73	- 0.66
7	0.29	0.44	- 0.07
8	0.21	0.17	- 0.25
9	0.02	0.23	- 0.38
Average Error	0.64	0.53	0.52

TABLE 4.2
(Continued)

Reading Number	Displacement Error, %	Overall Force Error, %	Friction Force Error, %
Run Number 3			
1	- 1.93	- 0.62	- 0.50
2	- 0.75	0.83	1.99
3	- 0.22	0.21	1.16
4	0.14	1.14	0.75
5	- 0.04	0.79	1.49
6	0.57	0.62	1.16
7	- 0.13	0.56	0.21
8	- 0.16	0.83	0.12
9	- 0.13	0.62	0.61
Average Error	0.45	0.69	0.89
Run Number 4			
1	- 3.94	- 0.08	3.45
2	- 1.18	- 0.08	3.45
3	- 0.13	0.06	0.16
4	0.49	0.44	0.99
5	0.24	0.42	0.49
6	- 0.07	0.40	0.99
7	- 0.11	0.93	0.63
8	- 0.20	0.23	0.37
9	- 0.09	0.29	0.16
Average Error	0.72	0.32	1.19
Run Number 5			
1	- 0.99	0	2.94
2	0.38	- 0.41	0.49
3	0.32	0.55	1.31
4	0.48	0	1.72
5	0.19	0	0
6	0.06	0.48	- 0.33
7	- 0.04	0.12	0.84
8	- 0.21	0.47	0.49
9	- 0.16	0.05	0.22
Average Error	0.31	0.23	0.93

$$\% \text{ Error} = \frac{(\text{Reading Value} - \text{Calibration Value})}{\text{Calibration Value}} \times 100$$

$$\text{Average Error} = \frac{1}{9} \sum_{j=1}^{9} \text{Error}_j \text{ (Absolute Value)}$$

TABLE 4.2
(Continued)

SUMMARY

Average Displacement Error, %	0.52
Average Overall Force Error, %	0.47
Average Friction Force Error, %	0.89

CHAPTER V

THE DATA REDUCTION PROCEDURE

The raw experimental data were in digital form and corresponded to the total applied force, the friction force and the specimen deformation at ten points, taken at equal increments of the total applied force. The total and friction forces and the deformation were obtained by subtracting the "zero" digital count from the digital reading and then multiplying the result by the conversion constant, i.e.

$$T = (T^* - T_o^*)\, c_T \tag{5.1a}$$

$$F = (F^* - F_o^*)\, c_f \tag{5.1b}$$

$$D = (D^* - D_o^*)\, c_D \tag{5.1c}$$

where T^*, F^* and D^* are the digital values in counts corresponding to the total applied force, the friction force and the specimen deformation; T_o^*, F_o^*, and D_o^* are the digital values in counts at zero total applied force, friction force and specimen deformation and the conversion constants are c_T, pounds/count, c_f, pounds/count, and c_D, inches/count.

A correction was made for the lateral specimen deformation due to expansion of the constraint cylinder since the specimen was assumed to be in a state of one-dimensional strain. Another correction was made for the elastic deflection of the loading rams because the specimen deformation measurement included ram deflections. Figure 5.1 shows the

deformations of the specimen, constraint cylinder and loading rams due to the applied loads.

Assuming that the diametral strain at the inner diameter of the constraint cylinder is

$$\varepsilon = \left[P d_i^2 / \bar{E}(d_o^2 - d_i^2) \right] \left[(1 - \nu) + (1 + \nu)(d_o^2 / d_i^2) \right] \qquad (5.2)$$

where d_i, d_o, $\bar{E}$ and ν are the internal diameter, external diameter, Young's modulus and Poisson's ratio of the constraint cylinder. The internal pressure change, P, was assumed to be the average normal stress, $(4T - 2F)/\pi d_i^2$. Loading ram deflections were determined from

$$\Delta L_1 = 4TL_1/\pi d^2 \bar{E} \qquad (5.3a)$$

$$\Delta L_2 = 4(T - F)L_2/\pi d^2 \bar{E} \qquad (5.3b)$$

where d, L_1, L_2 and $\bar{E}$ are the diameter, lengths and Young's modulus of the loading rams. Specimen volume after the corrections for elastic deflections of the constraint cylinder and loading rams are included is

$$V^* = (\pi/4) \left[d_i (1 + \varepsilon) \right]^2 (L_o - D + \Delta L_1 + \Delta L_2) \ . \qquad (5.4)$$

Then the one-dimensional-strain deformation of the specimen becomes

$$\Delta L = L_o - (1 + \varepsilon)^2 (L_o - D + \Delta L_1 + \Delta L_2) \qquad (5.5)$$

where D is the measured deflection obtained from equation (5.1c).

Because the distribution of the friction force along the length of the test specimen is unknown, the effective stress acting throughout the test specimen was assumed to be the average of the stresses acting on the specimen,

$$P = (4T - 2F)/\pi d_i^2 \ . \qquad (5.6)$$

The friction forces were normalized with respect to specimen length

and expressed as a per cent of the total applied force such that the normalized friction force ratio, F^{**}, is

$$F^{**} = 100\, F/TL_o \quad . \tag{5.7}$$

The Murnaghan representation of the experimental isothermal data was determined by a least-squares fit of the experimental data points. The volume ratio, v_o/v, of the Murnaghan equation can be expressed as

$$v_o/v = 1/(1 - \Delta L/L_o) = 1/(1 - \epsilon) \tag{5.8}$$

for the one-dimensional-strain state. A Murnaghan equation of the form

$$P = (B/A \left| \left[1/(1 - \epsilon)\right]^A - 1 \right| \tag{5.9}$$

was used to obtain the least squares residual, C of n experimental data points, (ϵ_i, P_i), with respect to the Murnaghan equation such that

$$C = \sum_{i=1}^{n} \left| (B/A) \left| \left[1/(1 - \epsilon_i)\right]^A - 1 \right| - P_i \right|^2 \quad . \tag{5.10}$$

A minimum value of the least squares residual, C, can be obtained by minimizing the residual with respect to the Murnaghan constants, A and B; therefore,

$$(\partial C/\partial A) = \sum_{i=1}^{n} 2 \left| B\left[1/(1 - \epsilon_i)\right]^{A-1} - (B/A^2)\left|\left[1/(1 - \epsilon_i)\right]^A - 1\right|\right|$$

$$\left|(B/A) \left| \left[1/(1 - \epsilon_i)\right]^A - 1\right| - P_i \right| = 0 \tag{5.11}$$

$$(\partial C/\partial B) = \sum_{i=1}^{n} 2 \left|(1/A)\left|\left[1 - /(1 - \epsilon_i)\right]^A - 1\right|\right|$$

$$\left|(B/A)\left| \left[1/(1 - \epsilon_i)\right]^A - 1\right| - P_i \right| = 0 \quad . \tag{5.12}$$

Because an explicit simultaneous solution of equations (5.11) and (5.12) could not be obtained, an iterative process was used to determine the A and B values. The iterative procedure utilized equation (5.10) and a rearranged version of equation (5.12) ,

$$B = A \sum_{i=1}^{n} P_i \left| \left[1/(1 - \epsilon_i) \right]^A - 1 \right| / \sum_{i=1}^{n} \left| \left[1/(1 - \epsilon_i) \right]^A - 1 \right|^2 \quad (5.12a)$$

to converge on the A and B values in the following manner. A value of A less than the correct value was assumed and B was computed with equation (5.12a), then the least squares residual, C, was computed with equation (5.10). The exponent A was increased by an increment, ΔA, and the new values of B and C were computed. This procedure was repeated until a minimum residual value, C_k, was obtained, then the increment ΔA was reduced to $\Delta A/10$ and the iterative process was repeated starting with A set equal to A_{k-2}. Successive tenfold decreases in the increment ΔA, followed by the application of the iterative minimization process permitted the value of A to be determined within $\pm \Delta A_{min}$. The tolerance on the Murnaghan exponent, A, was ± 0.0001 for each individual test. The iterative computations were carried out on a GE 235 time sharing digital computer for the isothermal data and the transformed Hugoniot data. A listing of the computer program is contained in Appendix A.

The least-squares fitting technique for discrete data points was used to determine the Murnaghan constants, A and B, for each test specimen. A composite Murnaghan equation for each series of specimens of the same nominal length was obtained by a least-squares fit of the series' individual Murnaghan equations. The fit was made to the individual Murnaghan equations rather than the discrete data points so that convergence difficulties could be minimized.

A least-squares residual, C_j, for each specimen's Murnaghan equation with respect to the composite Murnaghan equation over the interval, $[0, \epsilon_o]$, was expressed as

$$C_j = \int_0^{\epsilon_0} \left| (S/R) \left| \left[1/(1 - \epsilon) \right]^R - 1 \right| - (B_j/A_j) \right.$$

$$\left. \left| \left[1/(1 - \epsilon_1) \right]^{A_j} - 1 \right| \right|^2 d\epsilon \qquad (5.13)$$

where R and S are the constants of the composite Murnaghan equation.

Integration of equation (5.13) yielded

$$C_j = (S^2/R^2) \left| \left| \left[1 - (1 - \epsilon_0)^{1-2R} \right] / (1 - 2R) - 2 \left[1 - (1 - \epsilon_0)^{1-R} \right] / (1 - R) \right. \right.$$

$$\left. + \epsilon_0 \right| - (2SB_j/RA_j) \left| \left[1 - (1 - \epsilon_0)^{1-R-A_j} \right] / (1 - R - A_j) - \left[1 - (1 - \epsilon_0)^{1-R} \right] \right.$$

$$/(1 - 12) - \left[1 - (1 - \epsilon_0)^{1-A_j} \right] / (1 - A_j) + \epsilon_0 \left| + (B_j^2/A_j^2) \right.$$

$$\left| \left[1 - (1 - \epsilon_0)^{1-2A_j} \right] / (1 - 2A_j) - \left[1 - (1 - \epsilon_0)^{1-A_j} \right] \right.$$

$$\left. / (1 - A_j) + \epsilon_0 \right| \qquad (5.14)$$

Therefore, the least-squares residual, C, for n different individual Murnaghan equations became

$$C = \sum_{j=1}^{n} C_j \quad . \qquad (5.15)$$

Minimization of the least-squares residual, C, was obtained by requiring

$$(\partial C/\partial S) = -(2/R) \sum_{j=1}^{n} \left| (B_j/A_j) \left[u_1 - u_2 - u_3 + \epsilon_0 \right] \right| + (2S/R^2)$$

$$\sum_{j=1}^{n} \left[u_4 - 2u_3 + \epsilon_0 \right] = 0 \quad . \qquad (5.16)$$

and

$$(\partial C/\partial R) = (2S/R^3) \sum_{j=1}^{n} \left| (B_j(A_j) \left[u_1 - u_2 - u_3 + \epsilon_0 \right] \right| - (2S/R) \sum_{j=1}^{n}$$

$$\left| (B_j/A_j) \left[(u_5 - u_6) \ln (1 - \epsilon_0) + u_7 - u_8 \right] \right| - (2S^2/R^3) \sum_{j=1}^{n}$$

$$\left[u_4 - 2u_3 + \epsilon_0 \right] + (2S^2/R^2) \sum_{j=1}^{n} \left| \left[(u_{11} - u_6) \ln (1 - \epsilon_0) + u_9 - u_8 \right] \right|$$

$$- (2/R)(\partial S/\partial R) \sum_{j=1}^{n} \left| (B_j/A_j) \left[u_1 - u_2 - u_3 + \epsilon_o \right] \right| + (2S/R^2)$$

$$(\partial S/\partial R) \sum_{j=1}^{n} \left[u_4 - 2u_3 + \epsilon_o \right] \tag{5.17}$$

where

$$u_1 = \left[1 - (1 - \epsilon_o)^{1 - R - A_j} \right] / (1 - R - A_j) \tag{5.18a}$$

$$u_2 = \left[1 - (1 - \epsilon_o)^{1 - A_j} \right] / (1 - A_j) \tag{5.18b}$$

$$u_3 = \left[1 - (1 - \epsilon_o)^{1 - R} \right] / (1 - R) \tag{5.18c}$$

$$u_4 = \left[1 - (1 - \epsilon_o)^{1 - 2R} \right] / (1 - 2R) \tag{5.18d}$$

$$u_5 = \left[1 - (1 - \epsilon_o)^{1 - R - A_j} \right] / (1 - R - A_j) \tag{5.18e}$$

$$u_6 = (1 - \epsilon_o)^{1 - R} / (1 - R) \tag{5.18f}$$

$$u_7 = u_5 / (1 - R - A_j) \tag{5.18g}$$

$$u_8 = u_3 / (1 - R) \tag{5.18h}$$

$$u_9 = u_4 / (1 - 2R) \tag{5.18i}$$

$$u_{10} = \left[1 - (1 - \epsilon_o)^{1 - 2A_j} \right] / (1 - 2A_j) \tag{5.18j}$$

$$u_{11} = (1 - \epsilon_o)^{1 - 2R} / (1 - 2R) \tag{5.18k}$$

Equation (5.16) was solved to obtain the composite constant, S, such that

$$S = R \sum_{j=1}^{n} \left| (B_j/A_j) \left[u_1 - u_2 - u_3 + \epsilon_o \right] \right| / \sum_{j=1}^{n} \left[u_4 - 2u_3 + \epsilon_o \right] \tag{5.19}$$

and the derivative, $(\partial S/\partial R)$, was determined to be

$$(\partial S/\partial R) = \sum_{j=1}^{n} \left| (B_j/A_j) \left[u_1 - u_2 - u_3 + \epsilon_o \right] \right| / \sum_{j=1}^{n} \left[u_4 - 2u_3 + \epsilon_o \right]$$

$$+ R \sum_{j=1}^{n} \left| (B_j/A_j) \left[(u_5 - u_6) \ln (1 - \epsilon_o) + u_7 - u_8 \right] \right|$$

$$/ \sum_{j=1}^{n} \left[u_4 - 2u_3 + \epsilon_o \right] \tag{5.20}$$

Substitution of equivalent expressions for S and $(\partial S/\partial R)$ defined by equations (5.19) and (5.20) into equations (5.15) and (5.17), permitted the least-squares residual, C, and its derivative, $(\partial C/\partial R)$, to be expressed as functions of R but they were independent of S. Since equations (5.19) and (5.20) define S and $(\partial S/\partial R)$ as functions of R, the least-squares residual, C, could be minimized simultaneously with respect to R and S by variation of only R.

An iterative procedure was used to evaluate the constants, R and S, of the composite Murnaghan equation. The initial value, R_1, was assumed for the composite Murnaghan exponent and the least-squares residual, C, and the partial derivative, $(\partial C/\partial R)$, were computed after S and $(\partial S/\partial R)$ were determined with equations (5.19) and (5.20). An increment, ΔR, equal to $R_1/10$, was used to obtain the next R value,

$$R_m = R_{m-1} + \Delta R \left| (\partial C/\partial R)/(\partial C/\partial R) \right| \qquad (5.21)$$

and then the residual, C, and the partial derivative, $(\partial C/\partial R)$, were computed. The iteration was stopped when the difference between two successive R values was less than 0.0001. Composite Murnaghan equations were determined for the isothermal and Hugoniot sets of individual Murnaghan equations for each specimen series. Computations were made with a GE 235 time sharing digital computer. The computer program, LSMF-5, is presented in Appendix B.

All friction force values were adjusted to the nearest of ten normal force values, 3000, 6000, 9000, 12,000, 15,000, 18,000, 21,000, 24,000, 27,000 and 30,000 pounds, by assuming the friction force-normal force relationship in the vicinity of the ten normal force values to be linear.

Table 5.1 contains the polymethylmethacrylate property values, density, specific volume, coefficient of thermal expansion, and specific heat values that were used to compute the pressure offsets between the isothermal and Hugoniot states.

TABLE 5.1

POLYMETHYLMETHACRYLATE (PMMA) PROPERTY DATA

*Rohm and Haas Plexiglas Type 1A UVA	
*Density	0.04254 lb/in^3
*Specific Gravity	1.18
*Specific Volume	23.66 $in^3/lb.$
*Coefficient of Thermal Expansion	0.000135 in^3/in^3 °F
*Specific Heat at Constant Volume	0.33 BTU/lb °F
	3079 in-lb/lb °F
*Temperature	75°F
	534.7 °R
**Longitudinal Velocity	109500 in./sec.
**Shear Velocity	55120 in./sec.
**Bulk Velocity	89050 in./sec.

---

*Data from Rohm and Haas

**Data from Laboratory Measurements

CHAPTER VI

TEST RESULTS

The composite isothermal and the transformed Hugoniot stress-strain curves under one-dimensional strain conditions for each of the six specimen series are presented in Figure 6.1 and the corresponding Murnaghan constants are tabulated in Table 6.1. The isothermal composite curve and the data points from each test specimen series' individual tests are plotted in Figures 6.2, 6.3, 6.4, 6.5, 6.5 and 6.7. The specimen stress was assumed to be the average of the normal stresses acting on the two specimen boundaries. Results of the individual tests of each specimen series are summarized in Tables 6.4, 6.5, 6.6, 6.7, 6.8, and 6.9. Specimen geometry, expressed as the length-to-diameter ratio, affected the stress-strain curves. An increase in the specimen length produced a decrease in the specimen strain. The specimen strain of the isothermal composites at a stress of 150,000 lb/in^2, varied from 0.2848 for the 1/16-inch long series to 0.1138 for the 2-inch long specimen series. These values are plotted in Figure 6.8. The scatter of the individual test specimens is also shown in Figure 6.8.

A normal stress gradient was present in the test specimen due to the axial friction forces caused by the lateral constraint of the specimen. The magnitude of the friction force acting on an individual test specimen was dependent on the specimen length and the normal force

acting on the specimen. Observed minimum and maximum friction forces were 63 pounds produced by a 3000-pound normal force acting on a 1/16-inch long specimen, and 11,122 pounds produced by a 30,000 pound normal force acting on a 2-inch long specimen. A consistent relationship existed between the normalized friction force, F^{**}, and the applied normal force, T, for each of the test specimen series. Figure 6.3 shows the average normalized friction of each specimen series and the average value of all specimen series as the applied normal force was increased from 3000 to 30,000 pounds. Values of the average normalized friction forces and the minimum and maximum variation of the individual normalized friction forces are listed in Table 6.2.

Since the friction force distribution along the length of the specimen was not determined, the distribution of the normal stress gradient throughout the specimen was unknown and the specimen deformation could not be related to a specific normal stress. The range in the isothermal Murnaghan constants associated with the normal stress uncertainty is illustrated by Figures 6.4 and tabulated in Table 6.3.

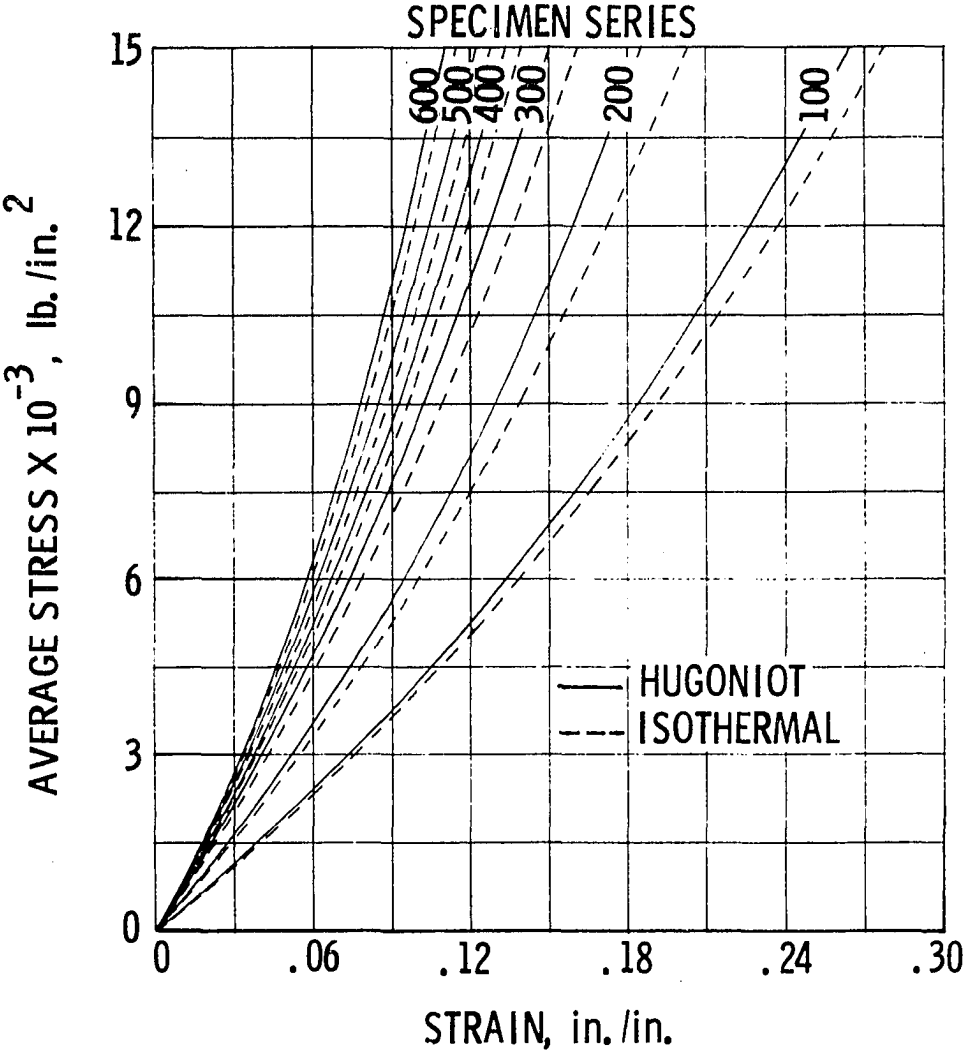

Figure 6.1 Composite Isothermal and Hugoniot stress-strain curves for the six specimen series

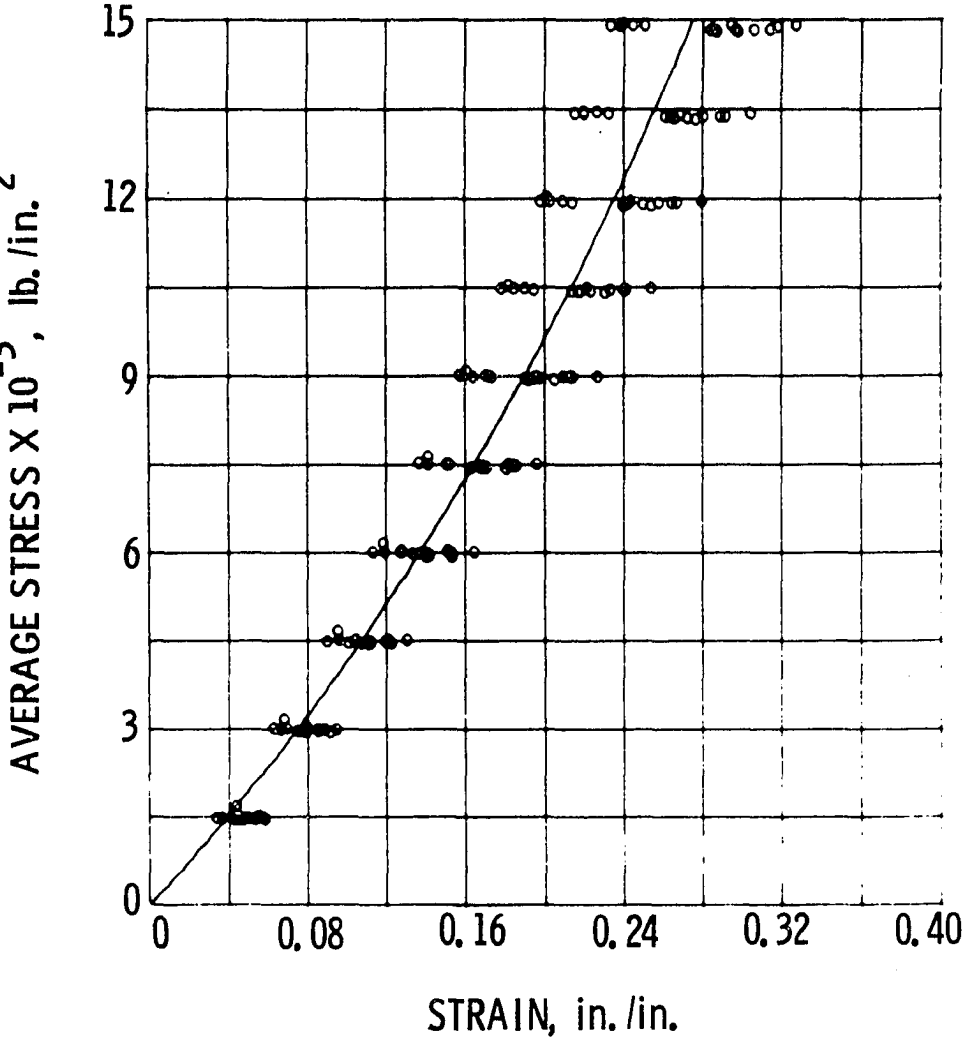

Figure 6.2 100 Series Isothermal composite and individual test data points

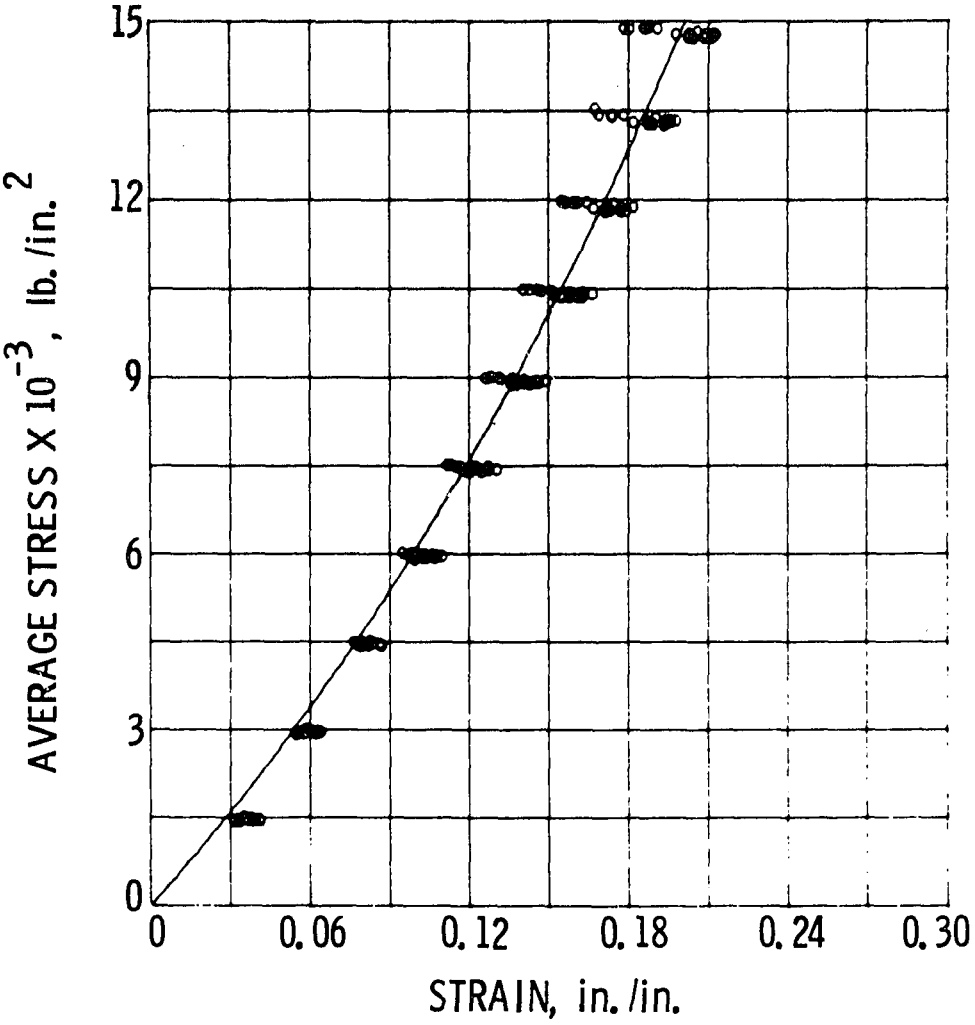

Figure 6.3 200 Series Isothermal composite and individual test data points

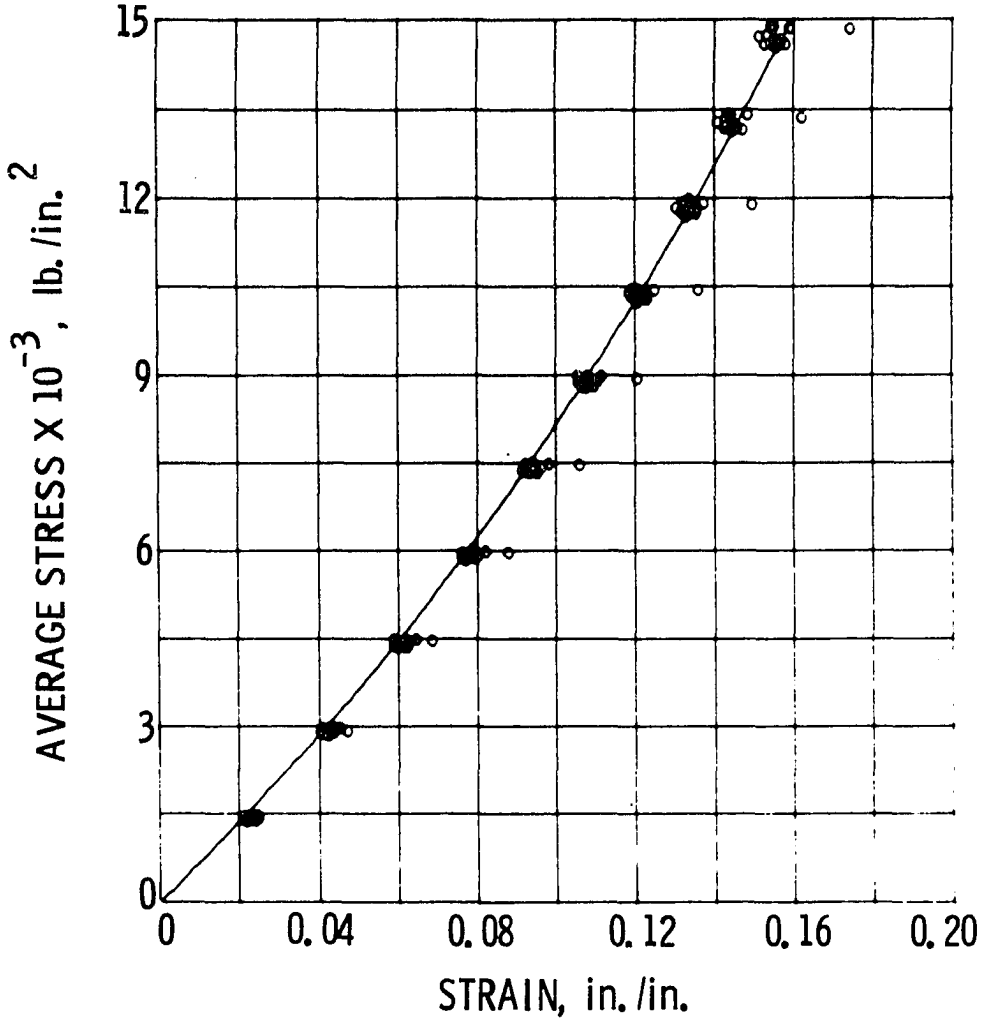

Figure 6.4 300 Series Isothermal composite and individual test data points

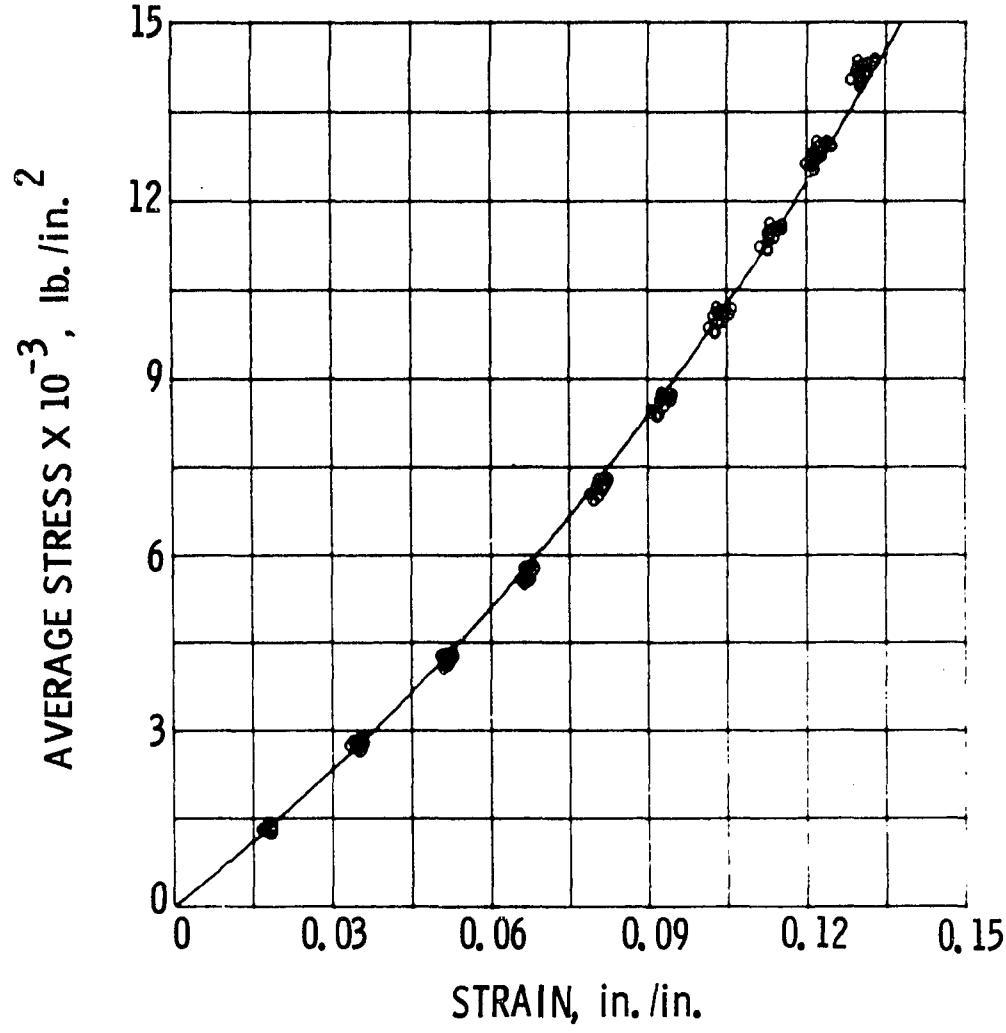

Figure 6.5 400 Series Isothermal composite and individual test data points

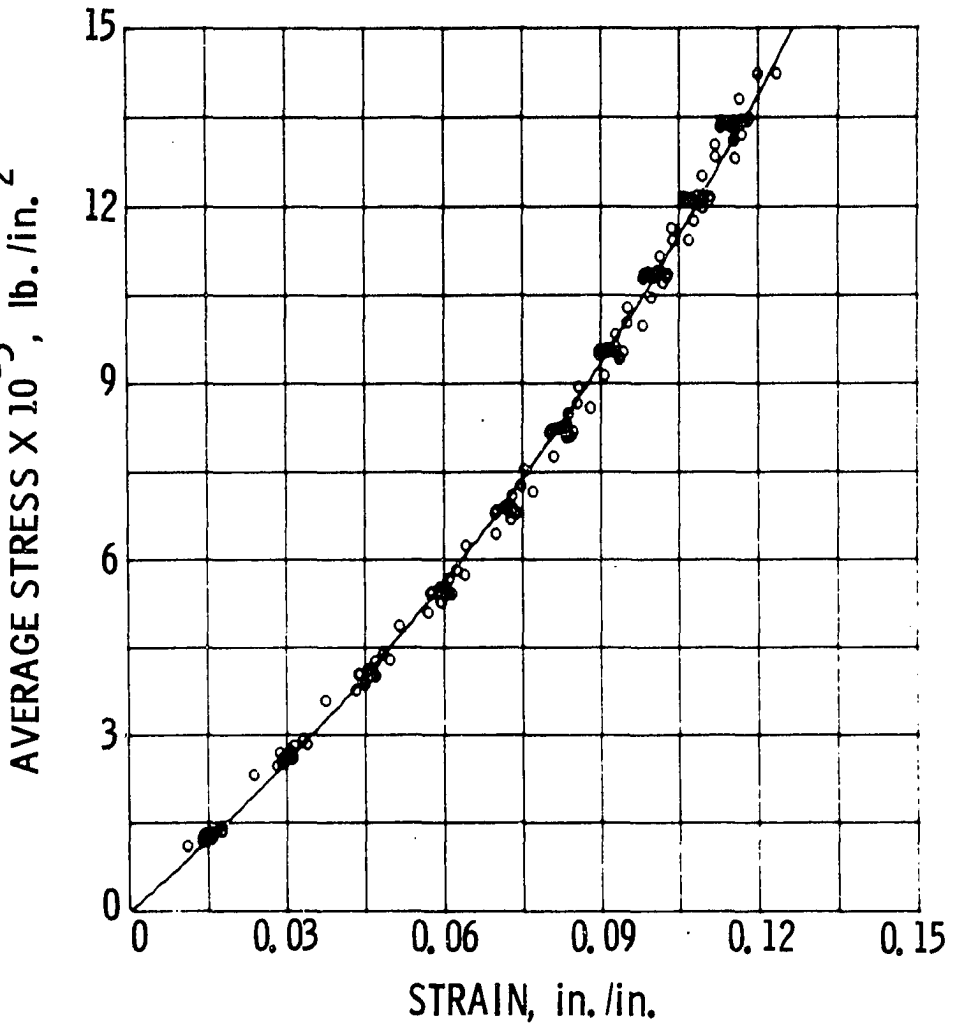

Figure 6.6 500 Series Isothermal composite and individual test data points

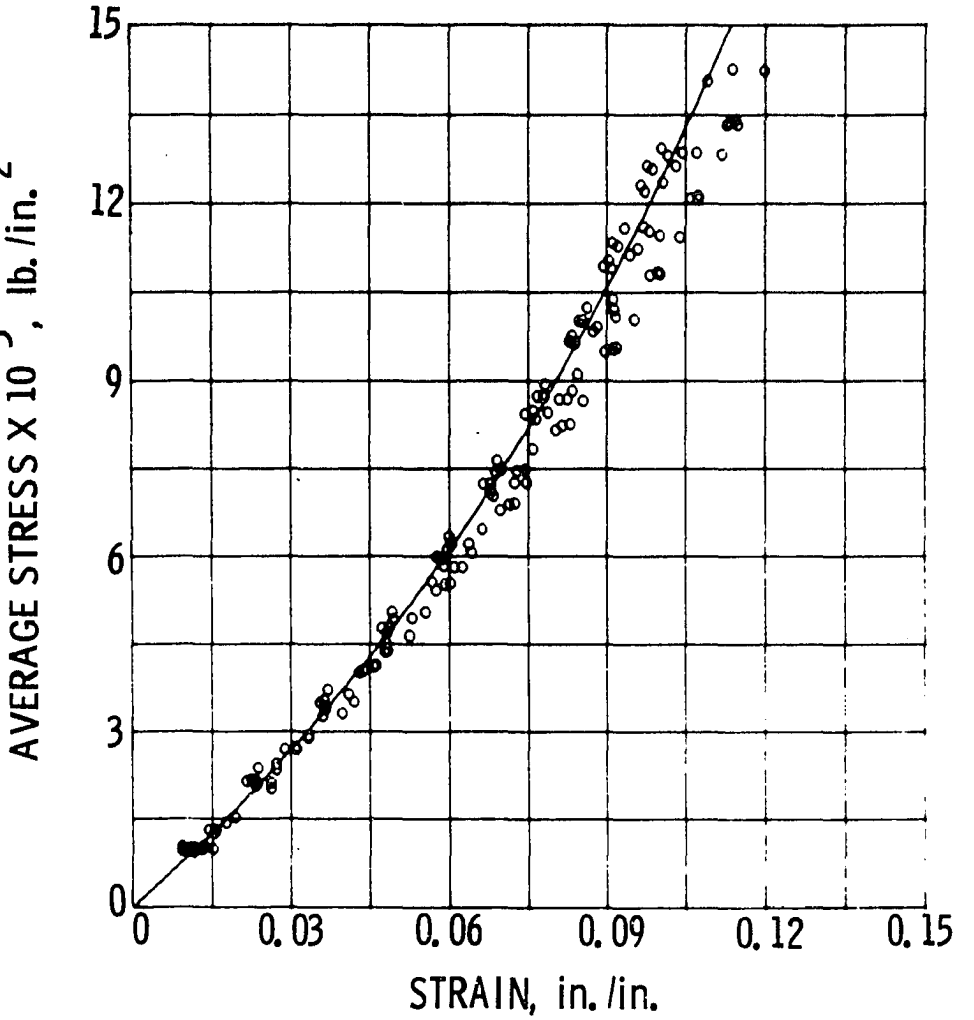

Figure 6.7 600 Series Isothermal composite and individual test data points

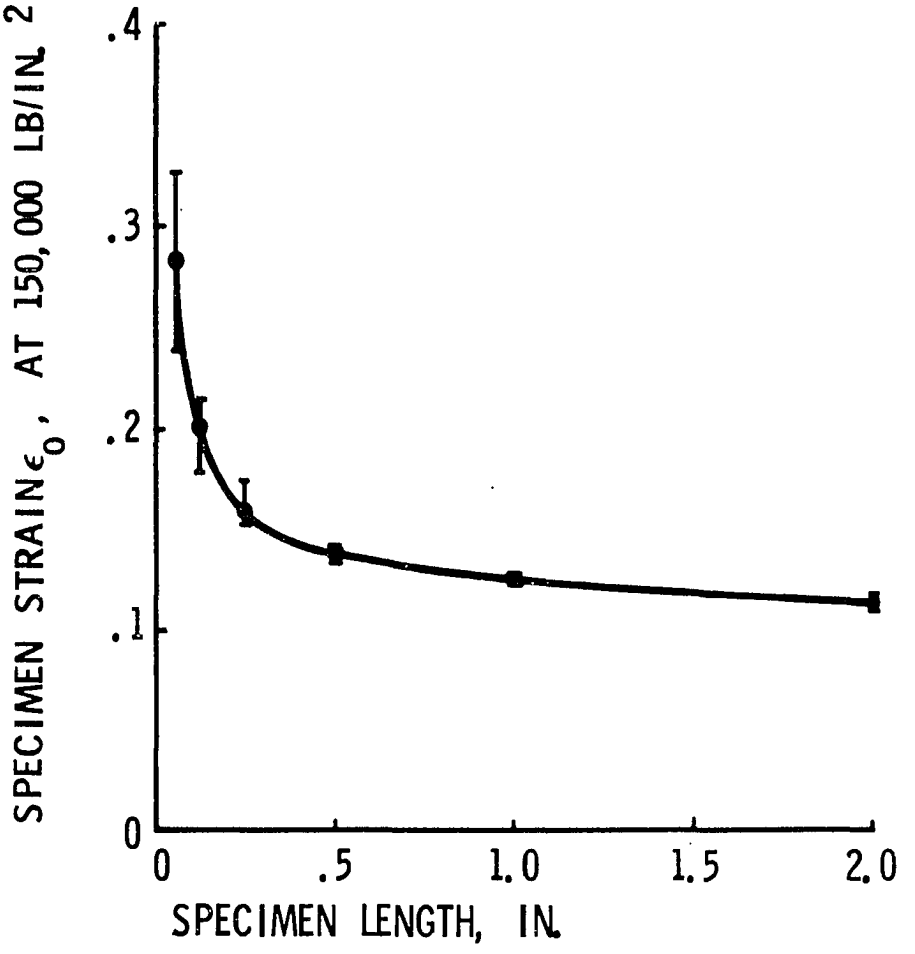

Figure 6.8 Composite isothermal strain at an average normal stress of 150,000 lb./in.^{2} vs. specimen length

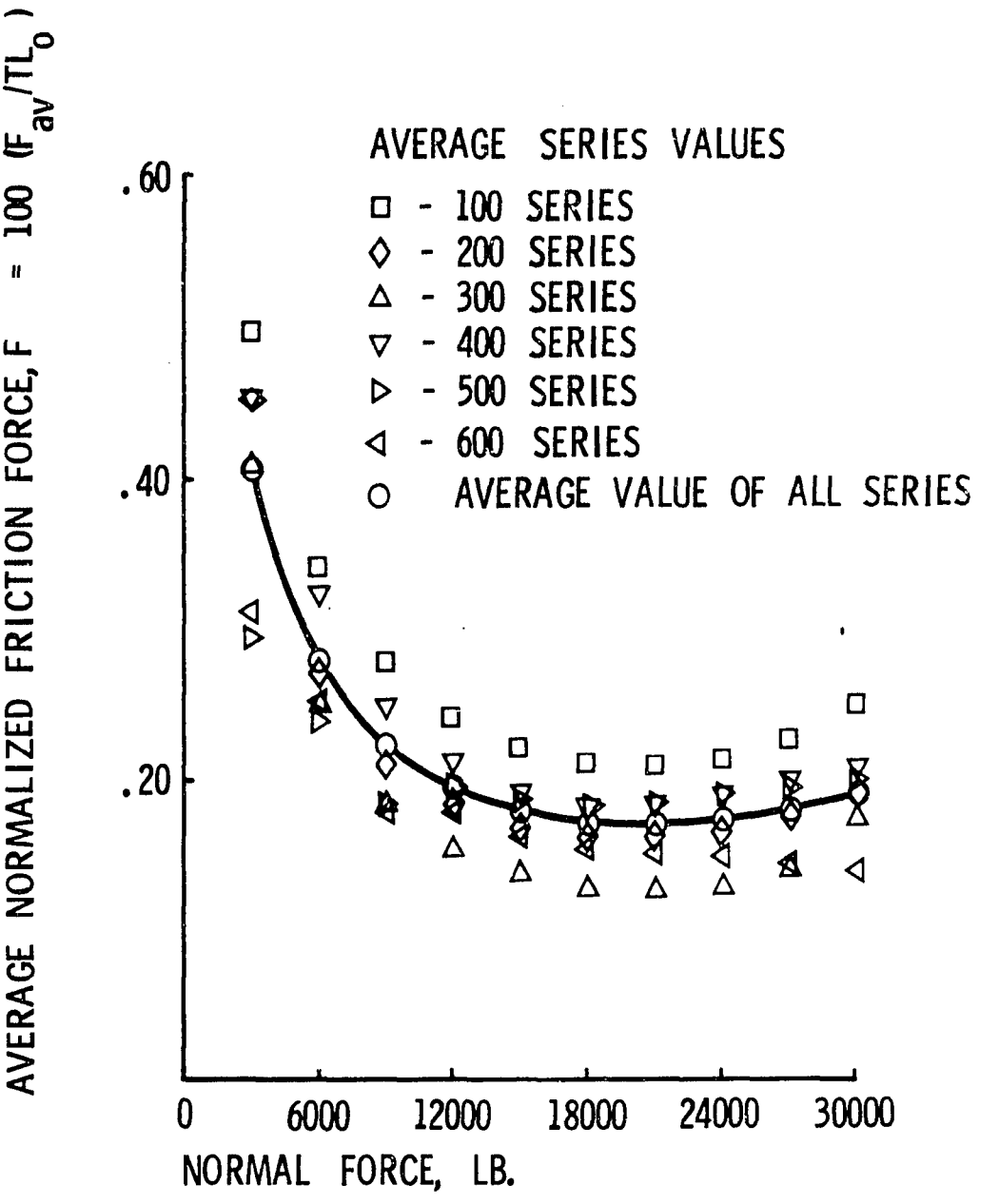

Figure 6.9 Average normalized friction force vs. applied normal force

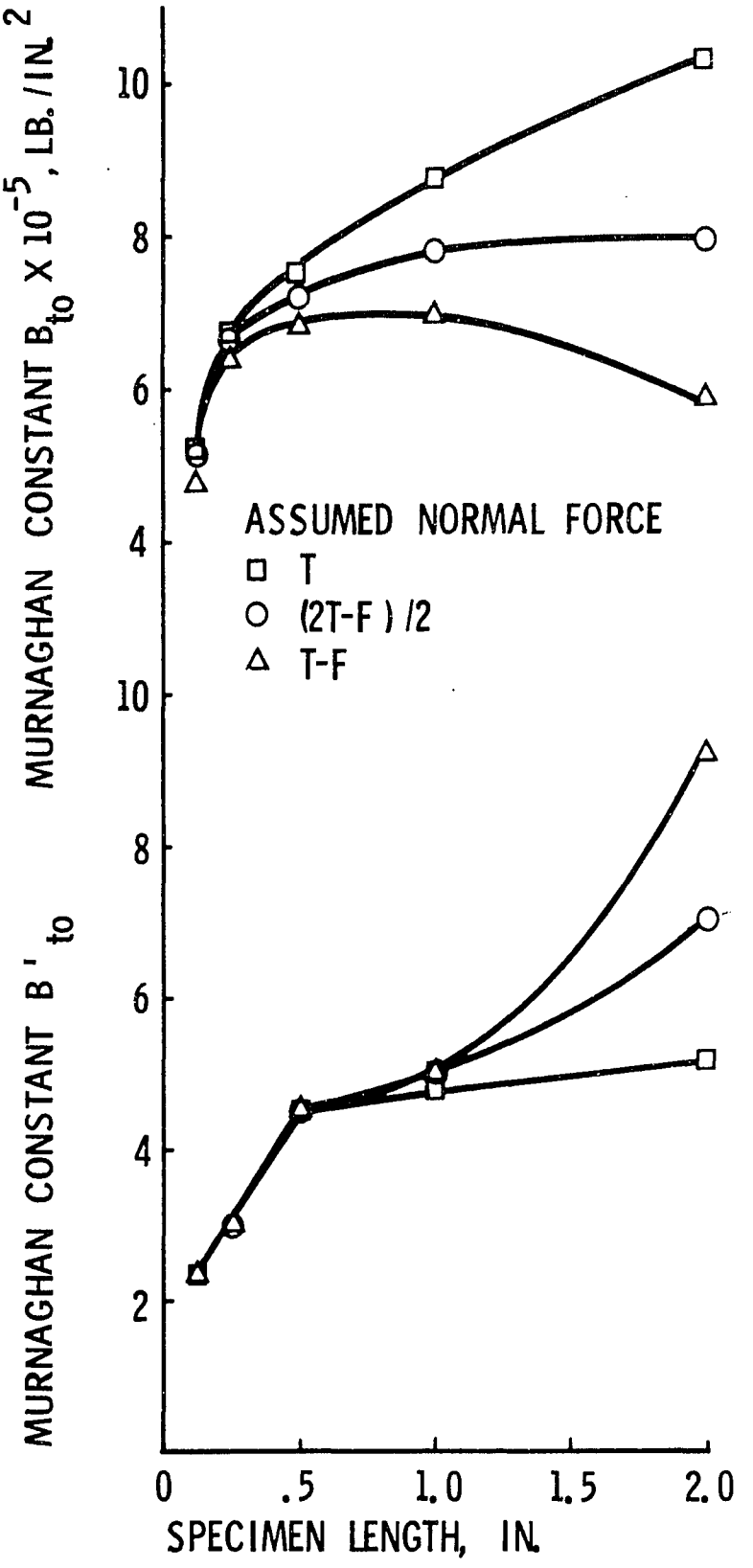

Figure 6.10 Variation of the isothermal Murnaghan constants due to friction

TABLE 6.1

POLYMETHYLMETHACRYLATE (PMMA) COMPOSITE SUMMARY

PMMA Specimen Series	Murnaghan Constant B_o	Murnaghan Constant B_o, lb/in^2.	ε_o, Strain at σ = 150,000 lb/in^2
	Isothermal Composites		
100	1.458	366000	0.2848
200	2.286	511700	0.2010
300	2.974	659800	0.1594
400	4.404	717200	0.1378
500	4.996	776000	0.1265
600	6.997	792300	0.1136
	Hugoniot Composites		
100	1.874	364700	0.2628
200	3.391	511000	0.1843
300	3.667	679100	0.1494
400	5.101	717100	0.1327
500	5.732	776500	0.1219
600	7.714	793400	0.1101

TABLE 6.2

POLYMETHYLMETHACRYLATE (PMMA) FRICTION SUMMARY

PMMA Specimen Series	100	200	300	400	500	600	Average	Total Normal Force, lb
Average Normalized Friction Force*, F**	49.6 -16.0a 11.9b	45.1 -14.1 8.8	40.8 -29.7 19.6	45.4 -17.3 17.7	29.5 -24.1 10.8	32.2 -24.5 6.3	40.4	3000
	33.9 -15.8 16.0	27.1 -10.2 12.1	24.7 -17.1 22.1	32.4 - 7.1 16.8	23.9 -18.5 21.3	25.3 -20.3 6.7	27.9	6000
	27.7 - 8.8 18.3	21.0 - 9.9 9.8	18.4 -11.8 9.4	24.9 - 9.8 15.2	21.0 -15.0 20.3	20.4 -16.1 7.5	22.2	9000
	24.1 -13.3 18.2	18.3 -10.1 9.5	15.5 - 9.3 8.4	21.3 - 7.6 13.5	19.5 -12.7 18.6	17.8 -13.8 7.0	19.4	12000
	22.1 -12.4 16.5	16.9 - 7.0 9.5	13.7 - 7.5 8.5	19.3 - 6.3 13.3	18.7 -10.3 16.2	16.4 -12.3 7.3	17.9	15000
	21.0 -13.4 15.7	16.2 -10.1 9.5	12.8 - 7.3 8.5	18.3 - 6.6 11.0	18.4 -10.4 14.1	15.5 -11.4 4.5	17.0	18000
	20.8 -13.0 15.2	16.2 -10.5 9.3	12.6 - 7.6 8.7	18.3 - 6.6 9.8	18.6 - 8.6 11.6	15.1 -10.8 5.2	16.9	21000
	21.3 -12.5 12.2	16.6 -10.5 9.3	12.9 - 8.2 6.7	19.1 - 6.2 8.8	18.9 - 9.8 9.6	14.8 -10.4 4.8	17.3	24000
	22.6 -11.8 14.6	17.6 -10.6 9.1	13.8 - 9.1 8.7	19.8 - 5.0 8.4	19.4 - 9.8 6.1	14.5 - 9.8 4.6	18.0	27000
	24.9 -11.5 13.9	19.1 -10.3 8.8	15.0 - 9.6 8.9	20.8 - 4.5 7.3	19.9 - 9.8 6.2	13.9 - 9.0 4.6	18.9	30000

$* F^{**} = 100 \frac{F_{AV}}{TL}$

a Minimum variation from average

b Maximum variation from average

TABLE 6.3

POLYMETHYLMETHACRYLATE (PMMA) ISOTHERMAL SUMMARY

PMMA Specimen Series	Murnaghan Constant B'_{TO}	Murnaghan Constant B_{TO}, lb./in^2	ϵ_o, Strain at σ = 150000 lb./in^2	Assumed Normal Force, lb.
200	2.277	517800	0.1995	T
300	2.928	673200	0.1576	
400	4.396	750200	0.1337	
500	4.760	870600	0.1182	
600	5.126	1026000	0.1034	
200	2.286	511700	0.2010	$\frac{2T - F}{2}$
300	2.974	659800	0.1594	
400	4.404	717200	0.1378	
500	4.996	776000	0.1265	
600	6.997	792300	0.1136	
200	2.338	474600	0.2107	T - F
300	3.017	645100	0.1615	
400	4.538	680400	0.1417	
500	5.000	692600	0.1365	
600	9.160	582100	0.1239	

TABLE 6.4

POLYMETHYLMETHACRYLATE (PMMA) 100 SERIES SPECIMEN SUMMARY

PMMA Specimen Number	Murnaghan Constant B'_o	Murnaghan Constant B_o, lb./in.^{2}	Least Squares Fit Errors, % Average	Maximum	ϵ_o, Strain at σ = 150000 lb/in^2
	Isothermal				
101	2.319	368200	5.4	31.8	0.2493
102	1.613	451900	2.3	15.3	0.2334
103	1.658	438700	2.6	16.2	0.2373
104	2.065	411600	4.0	25.2	0.2379
105	2.814	356700	5.2	30.4	0.2423
106	0.686	382500	2.1	12.9	0.2934
107	1.158	298400	3.0	19.4	0.3271
108	0.764	338300	1.9	9.3	0.3174
109	1.209	328900	3.9	23.0	0.3046
110	0.889	335300	2.4	14.3	0.3138
111	0.331	411200	1.5	5.7	0.2913
112	1.676	311200	4.6	26.3	0.2976
113	0.789	369000	2.3	12.2	0.2971
114	1.306	359600	3.3	18.2	0.2832
115	1.249	359000	2.7	14.3	0.2855
	Isothermal Composite				
	1.458	366000	13.5	36.9	0.2848
	Hugoniot Composite				
	1.874	364700			0.2628

TABLE 6.5

POLYMETHYLMETHACRYLATE (PMMA) 200 SERIES SPECIMEN SUMMARY

PMMA Specimen Number	Murnaghan Constant B'_o	Murnaghan Constant B_o, lb./in.^{2}	Least Squares Fit Errors, % Average	Maximum	ε_o, Strain at σ = 150000 lb/in^2
	Isothermal				
201	4.605	470100	4.3	27.2	0.1782
202	4.822	451600	4.3	26.5	0.1799
203	4.021	466600	4.1	25.7	0.1864
204	4.358	451900	3.7	23.8	0.1856
205	4.551	423400	4.1	26.3	0.1902
206	2.891	431700	2.2	14.9	0.2138
207	2.719	469100	2.4	15.1	0.2055
208	2.791	444100	3.1	16.6	0.2117
209	2.461	482700	3.0	15.5	0.2061
210	2.418	464800	2.4	14.8	0.2122
211	2.781	492100	2.1	13.9	0.1981
212	2.471	491100	2.5	14.4	0.2035
213	3.051	438600	4.2	24.0	0.2088
214	2.197	507400	2.3	13.8	0.2037
215	2.426	470300	2.0	13.4	0.2104
	Isothermal Composite				
	2.286	511700	8.6	36.0	0.2010
	Hugoniot Composite				
	3.391	511000			0.1843

TABLE 6.6

POLYMETHYLMETHACRYLATE (PMMA) 300 SERIES SPECIMEN SUMMARY

PMMA Specimen Number	Murnaghan Constant B'_0	Murnaghan Constant B_0, lb./in.^{2}	Least Squares Fit Errors, % Average	Maximum	ϵ_0, Strain at σ = 150000 lb/in^2
	Isothermal				
301	3.403	658200	0.6	1.9	0.1552
302	4.081	616000	0.6	5.1	0.1556
303	4.050	616600	0.5	2.3	0.1558
304	4.351	575500	0.8	5.3	0.1599
305	3.278	557000	0.5	2.4	0.1755
306	3.851	607700	0.9	7.2	0.1593
307	3.587	643000	0.4	1.6	0.1559
308	3.501	637400	1.1	8.6	0.1577
309	3.605	633000	0.7	5.1	0.1574
310	3.813	602300	0.7	5.2	0.1606
311	3.470	644100	0.9	5.0	0.1569
312	3.525	630000	0.9	5.4	0.1588
313	4.161	626500	0.8	4.7	0.1531
314	4.504	596600	1.1	9.2	0.1548
315	4.140	593700	1.0	3.8	0.1588
	Isothermal Composite				
	2.974	659800	3.8	17.3	0.1594
	Hugoniot Composite				
	3.667	679100			0.1494

TABLE 6.7

POLYMETHYLMETHACRYLATE (PMMA) 400 SERIES SPECIMEN SUMMARY

PMMA Specimen Number	Murnaghan Constant B'_0	Murnaghan Constant B_0, lb./in.^{2}	Least Squares Fit Errors, % Average	Maximum	ε_0, Strain at σ = 150,00 lb/in^2
	Isothermal				
401	5.319	667500	1.2	4.0	0.1374
402	5.610	675100	0.7	2.3	0.1343
403	5.559	659100	0.7	2.8	0.1368
404	5.741	654700	1.0	4.1	0.1360
405	5.610	656000	0.8	3.0	0.1368
406	5.037	686300	2.0	6.0	0.1370
407	5.181	701000	1.9	6.4	0.1341
408	5.421	677000	0.7	2.7	0.1354
409	5.308	673800	1.4	5.0	0.1367
410	5.419	683100	0.8	2.8	0.1347
411	5.407	677500	1.4	4.2	0.1355
412	4.987	696100	0.9	3.7	0.1361
413	5.171	696100	1.8	6.9	0.1348
414	4.730	706500	1.6	6.2	0.1367
415	5.171	692700	1.9	6.5	0.1352
	Isothermal Composite				
	4.404	717200	2.0	11.5	0.1378
	Hugoniot Composite				
	5.101	717100			0.1327

TABLE 6.8

POLYMETHYLMETHACRYLATE (PMMA) 500 SERIES SPECIMEN SUMMARY

PMMA Specimen Number	Murnaghan Constant B'_0	Murnaghan Constant B_0, lb./in.^{2}	Least Squares Fit Errors, % Average	Maximum	ϵ_0, Strain at σ = 150000 lb/in^2
	Isothermal				
501	5.919	715200	3.5	19.0	0.1275
502	5.818	725800	3.5	17.0	0.1269
503	4.684	812800	4.6	20.9	0.1245
504	6.145	705200	1.9	6.0	0.1272
505	5.955	706600	1.4	5.3	0.1282
506	6.243	723800	2.1	9.1	0.1245
507	5.895	764400	1.9	7.6	0.1222
508	5.985	725200	1.5	5.4	0.1259
509	5.995	746500	1.7	6.7	0.1235
510	6.385	694600	2.4	9.8	0.1269
511	6.305	736400	2.4	9.3	0.1228
512	5.823	752900	1.7	6.0	0.1239
513	5.575	775600	2.9	11.1	0.1230
514	5.985	737900	2.1	6.6	0.1245
515	5.885	743800	1.5	5.4	0.1245
	Isothermal Composite				
	4.996	776000	3.0	25.8	0.1265
	Hugoniot Composite				
	5.732	776500			0.1219

TABLE 6.9

POLYMETHYLMETHACRYLATE (PMMA) 600 SERIES SPECIMEN SUMMARY

PMMA Specimen Number	Murnaghan Constant B'_0	Murnaghan Constant B_0, lb./in.^{2}	Least Squares Average	Least Squares Maximum	ϵ_0, Strain at σ = 150,000 lb/in^2
	Isothermal				
601	10.501	638300	1.9	7.7	0.1117
602	8.501	743500	2.5	10.5	0.1109
603	7.401	796600	4.1	14.8	0.1112
604	9.291	664500	1.6	6.4	0.1146
605	8.581	708400	1.6	6.2	0.1137
606	7.297	727900	1.0	3.8	0.1182
607	8.481	766600	1.9	6.5	0.1089
608	8.329	765200	2.4	12.5	0.1097
609	6.324	845800	3.1	16.0	0.1121
610	6.316	851200	4.1	25.1	0.1117
611	7.511	753200	1.5	5.2	0.1146
	Isothermal Composite				
	6.997	792300	5.2	34.6	0.1138
	Hugoniot Composite				
	7.714	793400			0.1101

CHAPTER VII

DISCUSSION

The stress-strain Hugoniot relations for one-dimensional strain that were obtained by transformation of the isothermal stress-strain results do not agree with the Hugoniot relations determined by shock measurements. Results of the investigations of Schmidt and Evans, Liddiard, and Halpin and Graham, as compiled by Van Thiel et al[63] gave the following strain values, 0.087, 0.085, and 0.087, at a stress of 150,000 lb/in^2. A recent investigation by Schuler[64] found the shock Hugoniot strain at a stress of 150,000 lb/in^2 to be 0.085. The transformed Hugoniot strain at an average normal stress of 150,000 lb/in^2 was 0.110.

Possible sources of the discrepancy are:

1. A constant error in measuring the specimen force and deformation.
2. A specimen deformation error due to the radial compression of the surface imperfection of the specimen and the molybdenum disulfide lubricant.
3. The slow loading rate precluded any increase in material strength due to strain rate effects.

---

[63] Van Thiel et al., "Compendium of Shock . . . ."

[64] Schuler, Private Communication

4. An error in computing the pressure offsets between the isothermal and Hugoniot states.

5. A specimen deformation error resulting from flow of the specimen into the radial clearance between the constraint cylinder and the loading ram.

Observed force and displacement calibration errors were less than one per cent. The contribution to the axial specimen strain resulting from the radial compression of the specimen surface and the lubricant is estimated to be less than 0.1 per cent.

The stress-strain behavior of polymethylmethacrylate is strain rate dependent. Holt, Green, Babcock and Kumar[65] showed that the yield strength of polymethylmethacrylate increased with the logarithm of the strain rate and the stress at strain values of 0.02 and 0.04 increased with strain rate. Schuler[66] observed a time-dependent decay in the stress amplitude of shock waves. The effect of strain rate was not considered when the pressure offsets between the isothermal and Hugoniot states were computed.

The procedure that was used to transform the isothermal stress-strain curve to the Hugoniot state could have introduced an error if an incorrect material property value was used. The effect of variation of the material properties, the initial specific volume, the specific heat, the thermal coefficient of expansion and temperature, on the pressure offset from the isothermal to the Hugoniot state, can be evaluated by rearranging Equation (3.34)

---

[65] Holt, D. L., Green, S. J., Babcock, S.G., and Kumar, A., General Motors Technical Center, Mars Technical Progress Report, July 1967.

[66] Schuler, Private Communication

$$\Delta P = \left(2B_{TO}/B'_{TO}\right)\left\{\left[(v_o/v) - B'_{TO}/(B'_{TO} - 1)\right](v_o/v)^{B'_{TO}} - 1 + 1/(B'_{TO} - 1) - \beta T_o B'_{TO}\left[1 - (v_o/v)\right]\right\}/\left\{2C_v v/\beta B_{TO} v_o^2 - \left[1 - (v/v_o)\right]\right\} . \quad (7.1)$$

and then differentiating to obtain the following-equations

$$(\partial \Delta P/\partial v_o) = (2B_{TO}/v)\left\{\left[(v_o/v) - 1\right](v_o/v)^{B'_{TO}-2} + \beta T_o\right\}/\left\{2C_v v/\beta B_{TO} v_o^2 - \left[1 - (v/v_o)\right]\right\} + \left[(\beta C_v + 2\beta B_{TO} v_o)v/\beta B'_{TO} v_o^3\right]\left\{\left[(v_o/v) - B'_{TO}/(B'_{TO} - 1)\right](v_o/v)^{B'_{TO}-1} + 1/\left(B'_{TO} - 1\right) - \beta T_o B'_{TO}\left[1 - (v_o/v)\right]\right\}/\left\{2C_v v/\beta B_{TO} v_o^2 - \left[1 - (v/v_o)\right]\right\}^2 \quad (7.2)$$

$$(\partial \Delta P/\partial C_v) = -\left(4v/\beta B'_{TO} v_o^2\right)\left\{\left[(v_o/v) - B'_{TO}/(B'_{TO} - 1)\right](v_o/v)^{B'_{TO}} - 1 + 1/(B'_{TO}) - \beta T_o B'_{TO}\left[1 - (v_o/v)\right]\right\}/\left\{2C_v v/\beta B_{TO} v_o^2 - \left[1 - (v/v_o)\right]\right\}^2 \quad (7.3)$$

$$(\partial \Delta P/\partial \beta) = -2T_o B_{TO}\left[1 - (v_o/v)\right]/\left\{2C_v v/\beta B_{TO} v_o^2 - \left[1 - (v/v_o)\right]\right\} + (4C_v v/\beta^2 B'_{TO} v_o)\left\{\left[(v_o/v) - B_{TO}/(B'_{TO} - 1)\right](v_o/v)^{B'_{TO}} + 1/(B'_{TO} - 1) - \beta T_o B'_{TO}\left[1 - (v_o/v)\right]\right\}/\left\{2C_v v/\beta B_{TO} v_o^2 - \left[1 - (v/v_o)\right]\right\}^2 \quad (7.4)$$

$$(\partial \Delta P/\partial T_o) = -2\beta B_{TO}\left[1 - (v_o/v)\right]/\left\{2C_v v/\beta B_{TO} v_o^2 - \left[1 - (v/v_o)\right]\right\} \quad (7.5)$$

Effects on the pressure offset of a one per cent increase in the initial specific volume, the specific heat, the thermal coefficient of expansion and the temperature were evaluated using equations (7.2), (7.3), (7.4) and (7.5). Results presented in Table 7.1 show the pressure offset to be sensitive to small variations in the initial specific volume. The average change in the pressure offsets was 17, 23, 27, 30, 33 and 36 per cent for the 100, 200, 300, 400, 500, and 600 series composites. The pressure offset was ten times more sensitive to a one per cent change in initial specific volume than any of the other properties, specific heat, thermal coefficient of thermal expansion or temperature.

Stress-strain curves should be independent of specimen geometry to insure a true representation of the material behavior. Specimen geometry affected the results of the laterally confined compression tests. When high stresses were applied, the specimen was extruded into the annular clearance between the loading ram and the constraint cylinder. This could cause an error in the specimen strain unless the extruded volume was much less than the initial specimen volume. By examining each specimen after testing, an estimate of 0.00002 in^3 was obtained for the extruded volume. An undesirable normal stress gradient in the specimen was produced by friction between the specimen and the constraint cylinder as the specimen deformed. Lengthening the specimen increased the normal stress gradient.

In the absence of friction effects, the strain, specimen deformation divided by initial specimen length, at a particular applied normal stress could be expected to decrease to a limiting and constant value

as the specimen length increased. The friction forces resulting from the lateral constraint did not permit the test specimen geometry to be determined in such a fashion. (See Figure 6.2).

The normal strain gradient in the test specimen varied with the applied normal stress and the specimen length. Minimum and maximum normal stress gradients were 2.11 per cent in a 1/16-inch long specimen at an applied normal stress of 14,880 lb/in^2 , and 37.1 per cent in a 2-inch long specimen at an applied normal stress of 150,000 lb/in^2. Had the normal stress distribution, $P_h(x)$, in the specimen been known, the specimen deformation, ΔL, could have been related to the stress distribution with the Murnaghan equation with the following equation,

$$\Delta L = \int_0^{L_o - \Delta L} \epsilon_x dx = \int_0^{L_o - \Delta L} \left| 1 - \left[(B'_{To}/B_{To}) P_h(x) + 1 \right]^{-1/B'_{To}} \right| dx, \qquad (7.6)$$

where the initial specimen length is L_o. The normalized friction force-applied normal force relationship from specimen series to specimen series was similar but contained considerable scatter. Individual normalized friction force values varied from 55.5 to 137.5 per cent of the overall average curve of all specimen series. The average of the normal stresses acting on the specimen boundaries was assumed to be the effective stress throughout the length of the specimen.

The work of Stevens[67] and Warfield[68] displayed two different approaches to problem of friction resulting from lateral constraint. Stevens placed a lead cover over the specimen and then applied a correction factor to the results. The correction factors were obtained

[67] Stephens, D. R. and Lilley, E.M., "Compressions of Isotropic..."

[68] Warfield, R.W., "Compressibility of Bulk ....."

by determining the corrections that must be made to the test results of a reference material to give the known isothermal stress-strain curve. Warfield apparently ignored the friction problem.

The average variation from the isothermal composite curve of each specimen series data points was 13.5, 8.6, 3.8, 2.0, 3.0, and 5.2 per cent for the 100, 200, 300, 400, 500, and 600 specimen series. The isothermal composite curves gave a representative description of the experimental data. (See Figures 6.2, 6.3, 6.4, 6.5, 6.6 and 6.7).

TABLE 7.1

SENSITIVITY OF THE PRESSURE OFFSET TO CHANGES IN INITIAL SPECIFIC VOLUME, SPECIFIC HEAT, COEFFICIENT OF THERMAL EXPANSION AND INITIAL TEMPERATURE

PMMA Composite Series	PER CENT CHANGE IN THE SENSITIVITY RATIOS* $\frac{\Delta P}{P_h}$	$\frac{\partial(\Delta P)}{\partial v_o}\frac{\Delta v_o}{P_h}$	$\frac{\partial(\Delta P)}{\partial C}\frac{\Delta C_v}{P_h}$	$\frac{\partial(\Delta P)}{\partial \beta}\frac{\Delta \beta}{P_h}$	$\frac{\partial(\Delta P)}{\partial T_o}\frac{\Delta T_o}{P_h}$
100	6.18 a	0.87	- 0.06	0.09	0.03
	3.04 b	0.75	- 0.03	0.06	0.03
	10.02 c	1.40	- 0.11	0.14	0.03
200	6.62	1.30	- 0.07	0.10	0.04
	3.96	1.05	- 0.04	0.07	0.04
	9.70	2.49	- 0.10	0.14	0.04
300	7.46	1.78	- 0.08	0.12	0.04
	4.92	1.37	- 0.05	0.09	0.04
	10.35	3.73	- 0.11	0.15	0.04
400	7.47	2.03	- 0.08	0.12	0.05
	5.23	1.52	- 0.05	0.10	0.04
	10.03	4.41	- 0.11	0.15	0.05
500	7.70	2.27	- 0.08	0.13	0.05
	5.58	1.66	- 0.06	0.11	0.04
	10.13	5.09	- 0.11	0.15	0.05
600	7.33	2.43	- 0.08	0.12	0.05
	5.60	1.74	- 0.06	0.11	0.04
	9.36	5.61	- 0.10	0.14	0.05

*For an assumed 1% change in initial specific volume, specific heat, coefficient of thermal expansion and initial temperature

a - average value

b - minimum value

c - maximum value

CHAPTER VIII

CONCLUSIONS AND RECOMMENDATIONS

Further development of the laterally constrained compression test is necessary before the technique can be used to obtain accurate isothermal data. The friction forces resulting from the lateral constraint of the specimen and the low maximum pressure limitation are the primary shortcomings of the laterally constrained compression test. The effects of friction resulting from the lateral constraint of the specimen cannot be neglected. Additional work is required to determine the normal stress distribution in the specimen and the variation of the normal stress distribution from specimen to specimen.

The Hugoniot stress-strain curves obtained by transforming the experimentally determined isothermal stress-strain curves did not agree with those obtained by shock measurements. The discrepancy is believed to be the result of the absence of strain rate effects, the effect of friction and the possible errors in computing the pressure offsets between the isothermal and Hugoniot states.

The material properties used to compute the pressure offsets between the isothermal and Hugoniot states must be known precisely if the pressure offsets are to be realistic. Small errors in the initial specific volume produce unacceptably large errors in the pressure offsets.

Care must be exercised in preparing the test specimen. All surfaces must be polished to a smooth finish that is free of scratches and machine tool marks. The ends of the specimen must be flat and parallel and normal to axis of the cylinder. Lubricants should not be used to coat the test specimen constraint cylinder or loading rams if the lubricant film is thick.

BIBLIOGRAPHY

Articles

Anderson, O.L. "The Use of Ultrasonic Measurements Under Modest Pressure to Estimate Compression at High Pressure," J. Phys. Chem. Solids, 27 (1966), pp. 547-65.

Barker, L.M. "Fine Structure of Compressive and Release Wave Shapes in Aluminum Measured by the Velocity Interferometer Technique," Proc. IUTAM Conf. on High Dynamic Pressures, Paris, France, September, 1967, (1968), pp. 483-505.

Barker, L.M. and Hollenbach, R.E. "System for Measuring the Dynamic Properties of Materials," Rev. Sci. Inst., 35 (1964), pp. 742-6.

Birch, F.J. "The Effect of Pressure Upon the Elastic Parameters of Isotropic Solids, According to Murnaghan's Theory of Finite Strain," J. Appl. Phys., 9 (1938), pp. 279.

Bradburn, M. "The Equation of State for a Face-Centered Cubic Lattice, Proc. Camb. Phil. Soc., 39 (1943), p. 113.

DiBenedetto, A.T. "Molecular Properties of Amorphous High Polymers, I. A Cell Theory for Amorphous High Polymers," J. Polymer Sci. A., 1 (1963), pp. 3459.

Drummond, W.E. "Explosive Induced Shock Waves, Part I. Plane Shock Waves," J. Appl. Phys., 28 (1957), p. 1437.

Duvall, G.E. "Pressure-Volume Relations in Solids," J. Appl. Phys., 27 (1957), pp. 235-38.

Duvall, G.E. and Zwolinski, B.J. "Entropic Equations of State and Their Application to Shock Phenomena in Solids," J. Acoust. Soc. Am., 27 (1955), pp. 1054-58.

Flory, P.J., Orwall, R.A. and Vrijo, A. "Statistical Thermodynamics of Chain Molecule Liquids, I. An Equation of State for Normal Paraffin Hydrocarbons," J. Am. Chem. Soc., 86 (1964), pp. 3507.

Fürth, R. "On the Equation of State for Solids," Proc. Roy. Soc., A183 (1944), pp. 87.

Graham, R.A., Neilson, F.W. and Benedick, W.B. "Piezoelectric Current from a Submicrosecond Stress Gage," J. Appl. Phys., 36 (1965), pp. 1775-83.

Koehler, J.S. and Duvall, G.E. "Shock Wave Data and the Closed Shell Repulsive Potential in the Noble Metals," Bull. Am. Phys. Soc. Ser. II, 4 (1959), p.-283.

Lazarus, D. "The Variation of the Adiabatic Elastic Constant of KCl, NaCl, CuZn, Cu, and AL with Pressure to 10,000 Bars," Phys. Rev., 76 (1949), p. 545.

McSkimin, H.J. and Andreatch, P., Jr. "Analysis of the Pulse Superposition Method of Measuring Ultrasonic Wave Velocities as a Function of Temperature and Pressure," J. Acoust. Soc. Am., 34 (1962), p. 609.

Misra, R.D. "On the Stability of Crystal Lattices. II," Proc. Camb. Phil. Soc., 36 (1940), p. 175.

Murnaghan, F.D. "The Compressibility of Media under Extreme Pressures," Proc. Natn. Acad. Sci., 30 (1944), p. 244.

Overton, W.C., Jr. "Relation Between Ultrasonically Measured Properties and the Coefficients in the Solid Equation of State," J. Chem. Phys., 37 (1962), pp. 116-19.

Pack, D.C., Evans, W.M. and James, H.J. "The Propagation of Shock Waves in Steel and Lead," Proc. Phys. Soc., 60 (1948), Part I.

Rotter, C.A. and Smith, C.S. "Ultrasonic Equation of State of Iron, I. Low Pressure, Room Temperature," J. Phys. Chem. Solids, 27 (1966), pp. 267-76.

Ruoff, A.L. "Linear Shock-Velocity-Particle-Velocity Relationship," J. Appl. Phys., 38 (1967), p. 4976.

Spencer, R.S. and Gilmore, G.P. "Equation of State for Polystyrene," J. Appl. Phys., 20 (1949), p. 504.

Stephens, D.R. and Lilley, E.M. "Compressions of Isotropic Lithium Hydrides," J. Appl. Phys., 39 (1968), pp. 177-80.

Walsh, J.M. and Christian, R.H. "Equation of State of Metals From Shock Wave Measurements," Phys. Rev., 97 (1955), p. 1544.

Warfield, R.W. "Compressibility of Bulk Polymers," Polymer Engr. and Sci., 6 (1966), pp. 176-80.

Whitaker, H.L. and Griskey, R.G. "A Generalized Equation of State for Polymers," J. Appl. Polymer Sci., 11 (1967), pp. 1001-8.

Reports

Doran, D.G. Measurement of Shock Pressures in Solids. Poulter Laboratories, Stanford Research Institute, Menlo Park, California, TR 002-63 (April 1963).

Van Thiel, et al. Compendium of Shock Wave Data. University of California, Lawrence Radiation Laboratory, Livermore, California, Vol. I and II (June 1966).

Warfield, R.W. The Compressibility of Polymers to 20000 Atmospheres. Naval Ordnance Laboratory NOLTR-66-45 (June 1966).

Williams, E.O. An Etched Manganin Gage System for Shock Pressure Measurement in a High Noise Environment. Instrument Society of America Preprint Number P7-2-PHYMMID-67 (Sept. 1967).

Books

Adler, B.J. Physics Experiments with Strong Pressure Pulses, in Solids Under Pressure. Edited by Paul and Warschauer. New York: Mc-Graw Hill, 1963.

Born, M. and Huang, K. Dynamic Theory of Crystal Lattices. Oxford: Clarendon Press, 1954.

Bridgman, P.W. The Physics of High Pressures. London, England: Bell and Sons, 1949.

Duvall, G.E. Some Properties and Applications of Shock Waves, in Response of Metals to High Velocity Deformation. Edited by Shewmon and Zackay. New York: Interscience, 1961.

Duvall, G.E. and Fowles, G.R. Shock Waves, in High Pressure Physics and Chemistry. Vol. 2. Edited by R. S. Bradley. New York: Academic Press, 1962.

Rice, M.H., McQueen, R.G. and Walsh, J.M. Compression of Solids by Strong Shock Waves, in Solid State Physics. Vol. 6. Edited by Seitz and Turnbull. New York: Academic Press, 1958.

Slater, J.C. Introduction to Chemical Physics. New York: McGraw-Hill, 1939.

APPENDIX A
COMPUTER PROGRAM LSMF-4 LISTING

LSMF-4

```
100 DIM A(125),B(125),C(125),D(12),E(10)
101 DIM U(12),V(12),X(10),Y(10),Z(10)
110 READ X0,Y0,N,I
111 READ D0,U0,V0
120 FOR J=1 TO N+1
130 READ D(J),U(J),V(J)
135 NEXT J
136 LET D(12)=D(1)
137 LET U(12)=U(1)
138 LET V(12)=V(1)
142 FOR J=2 TO N+1
144 LET D(J-1)=(D(J)-D(12))*D0
146 LET U(J-1)=(U(J)-U(12))*U0
148 LET V(J-1)=(V(J)-V(12))*V0
150 NEXT J
152 PRINT
154 PRINT "PMMA SPECIMEN ";I
156 PRINT
158 PRINT
160 PRINT "J","D(J)","U(J)","V(J)"
162 PRINT
164 FOR J=1 TO N
166 PRINT J,D(J),U(J),V(J)
168 NEXT J
170 PRINT
190 READ B1,B2,W,P,R1,R2
200 FOR J=1 TO N
210 LET Y(J)=(2*U(J)-V(J))/(2*Y0)
220 LET Q=Y(J)*R1↑2*(1-P+(1+P)*R2↑2/R1↑2)/(W*(R2↑2-R1↑2))
230 LET X(J)=D(J)/X0-(B1*U(J)+B2*(U(J)-V(J)))/(W*Y0*X0)
240 LET X(J)=1-(1-X(J))*(1+Q)↑2
250 NEXT J
370 PRINT
380 PRINT
390 LET L=1
400 IF L>1 THEN 430
410 PRINT "ISOTHERMAL VALUES"
420 GO TO 440
430 PRINT "HUGONIOT VALUES"
440 PRINT
450 PRINT
570 READ A0
571 IF L>1 THEN 590
575 READ A(1)
580 PRINT "K","A(K)","B(K)","C(K)"
590 PRINT
600 LET K=1
610 LET F0=0
620 LET G0=0
630 FOR J=1 TO N
```

LSMF-4 CONTINUED

```
640 LET U(J)=1/(1-X(J))
650 LET F0=F0+(U(J)↑A(K)-1)*Y(J)
660 LET G0=G0+(U(J)↑A(K)-1)↑2
670 NEXT J
680 LET B(K)=F0*A(K)/G0
690 LET C0=0
700 FOR J=1 TO N
710 LET C0=C0+((B(K)/A(K))*(U(J)↑A(K)-1)-Y(J))↑2
720 NEXT J
730 LET C(K)=C0
740 LET K=K+1
750 IF K>2 THEN 790
760 LET A(K)=A(K-1)+A0
770 GO TO 610
780 IF (C(K-1)-C(K-2))>0 THEN 810
790 LET A(K)=A(K-1)+A0
800 GO TO 610
810 LET A0=A0/10
820 IF A0<.0001 THEN 850
830 IF K>3 THEN 833
831 LET A(K)=A(K-2)+A0
832 GO TO 610
833 LET A(K)=A(K-3)+A0
840 GO TO 610
850 LET A=A(K-2)
860 LET B=B(K-2)
870 PRINT (K-2),A(K-2),B(K-2),C(K-2)
880 LET E=0
890 LET S=0
900 FOR J=1 TO N
910 LET Z(J)=(B/A)*((1/(1-X(J)))↑A-1)
920 LET E(J)=100*(Y(J)-Z(J))/Z(J)
930 LET E=E+ABS(E(J))
940 LET S=S+(ABS(E(J)))↑2
950 NEXT J
960 FOR J=1 TO N
970 FOR K=1 TO N
980 LET G=ABS(E(K))-ABS(E(J))
990 IF G>0 THEN 1020
1000 NEXT K
1010 GO TO 1030
1020 NEXT J
1030 LET E0=ABS(E(J))
1040 PRINT
1050 PRINT
1060 PRINT "J","X(J)","Y(J)","Z(J)","E(J)"
1070 PRINT
1080 FOR J=1 TO N
1090 PRINT J,X(J),Y(J),Z(J),E(J)
1100 NEXT J
```

LSMF-4 CONTINUED

```
1110 PRINT
1120 PRINT "E-MAX.=";E0
1130 PRINT "E-AV.=";(E/N)
1140 PRINT "E-STD.DEV.=";((S/N)↑.5)
1150 IF L>2 THEN 9999
1250 LET L=L+1
1260 READ C,S,T0,V0
1270 PRINT
1280 PRINT
1290 PRINT "C","S","T0","V0"
1300 PRINT
1310 PRINT C,S,T0,V0
1320 PRINT
1330 PRINT
1340 FOR J=1 TO N
1350 LET G=S*B/(1-X(J))
1360 LET F1=B*V0/(A*(A-1))*((1/(1-X(J)))↑(A-1)-1)
1370 LET F2=(B/A+S*B*T0)*V0*X(J)
1380 LET F=F1-F2
1390 LET D=(G*Y(J)*V0*X(J)/2-F)/C
1400 LET E=1-G*V0*X(J)/(2*C)
1410 LET Y(J)=Y(J)+D/E
1420 NEXT J
1430 LET L=L+1
1435 LET A(1)=A
1440 GO TO 400
1500 DATA X0,Y0,N,I
1510 DATA D0,U0,V0
1520 DATA D(1),U(1),V(1),------,D(N+1),U(N+1),V(N+1)
1530 DATA B1,B2,M,P,R1,R2
1540 DATA A0,A1
1550 DATA C,S,T0,V0
1560 DATA A0
9999 END
```

Program Input Parameters
Statement Number
1500
XO = Initial specimen length, in.
YO = Specimen area, $in.^2$
N = Number of data points minus one
I = Specimen identification
1510
DO = Displacement conversion constant, in./count
UO = Normal force conversion constant, lb./count
VO = Friction force conversion constant, lb./count
1520
D(J)= Digital value proportional to the specimen deformation, counts
U(J)= Digital value proportional to the normal force, counts
V(J)= Digital value proportional to the friction force, counts
1530
B1 = Length of upper loading ram, in.
B2 = Length of lower loading ram, in.
W = Young's modulus of constraint cylinder, $lb./in.^2$
P = Poisson's ratio for the constraint cylinder
R1 = Internal radius of the constraint cylinder, in.
R2 = External radius of the constraint cylinder, in.
1540
A0 = Assumed initial Murnaghan exponent increment
A1 = Assumed initial Murnaghan exponent (isothermal)
1550
C = Specific heat (constant volume) of the specimen $in.\text{-}lb/lb.\text{-}°R$
S = Coefficient of thermal expansion of the specimen $in.^3/in^3\text{-}°R$
T0 = Initial specimen temperature, °R
V0 = Initial specific volume of the specimen, $in.^3/lb.$
1560
A0 = Assumed initial Murnaghan exponent increment

APPENDIX B .
COMPUTER PROGRAM LSMF-5 LISTING

LSMF-5

```
100 DIM A(15),B(15),C(100),D(100)
101 DIM R(100),S(100),U(11),X(100),Y(100)
110 READ X0,N,I
120 READ R(1)
125 LET R0=ABS(R(1)/10)
130 LET L=1
140 PRINT "PMMA COMPOSITE SPECIMEN SERIES";I
150 PRINT
160 PRINT
170 FOR J=1 TO N
180 READ A(J),B(J)
190 NEXT J
200 IF L>1 THEN 230
210 PRINT "ISOTHERMAL VALUES"
220 GO TO 240
230 PRINT "HUGONIOT VALUES"
240 PRINT
250 LET M=1
260 PRINT "K","A(K)","B(K)","C(K)"
270 PRINT
280 LET F1=0
281 LET F2=0
282 LET F3=0
283 LET F4=0
285 LET F5=0
286 LET Z=LOG(1-X0)
287 LET Q=R(M)
290 FOR J=1 TO N
291 LET T=A(J)
300 LET U(1)=(1-(1-X0)↑(1-T-Q))/(1-T-Q)
310 LET U(2)=(1-(1-X0)↑(1-T))/(1-T)
320 LET U(3)=(1-(1-X0)↑(1-Q))/(1-Q)
330 LET U(4)=(1-(1-X0)↑(1-2*Q))/(1-2*Q)
340 LET U(5)=(1-X0)↑(1-T-Q)/(1-T-Q)
350 LET U(6)=(1-X0)↑(1-Q)
360 LET U(7)=U(5)/(1-T-Q)
370 LET U(8)=U(3)/(1-Q)
380 LET U(9)=U(4)/(1-2*Q)
390 LET U(10)=(1-(1-X0)↑(1-2*T))/(1-2*T)
400 LET U(11)=(1-X0)↑(1-2*Q)/(1-2*Q)
410 LET G1=U(1)-U(2)-U(3)+X0
420 LET G2=U(4)-2*U(3)+X0
430 LET G3=(U(5)-U(6))*Z+U(7)-U(8)
440 LET G4=(U(11)-U(6))*Z+U(9)-U(8)
450 LET G5=U(10)-2*U(2)+X0
460 LET F1=F1+B(J)*G1/T
470 LET F2=F2+G2
480 LET F3=F3+B(J)*G3/T
490 LET F4=F4+G4
500 LET F5=F5+B(J)↑2*G5/T↑2
```

Program Input Parameters
Statement Number
810
XO = Maximum specimen strain, in./in.
N = Number of specimen
I = Specimen series identification number
820
R(1)= Assumed initial Murnaghan exponent (isothermal)
830
A(J)= Murnaghan exponent (isothermal)
B(J)= Murnaghan constant, lb./in.^{2}(isothermal)
840
R(1)= Assumed initial Murnaghan exponent (Hugoniot)
850
A(J)= Murnaghan exponent (Hugoniot)
B(J)= Murnaghan constant, lb./in.^{2}(Hugoniot)